

Alma Mater Studiorum Università di Bologna
Archivio istituzionale della ricerca

Nectarine volatilome response to fresh-cutting and storage

This is the final peer-reviewed author's accepted manuscript (postprint) of the following publication:

Published Version:

Ceccarelli A., Farneti B., Khomenko I., Cellini A., Donati I., Aprea E., et al. (2020). Nectarine volatilome response to fresh-cutting and storage. *POSTHARVEST BIOLOGY AND TECHNOLOGY*, 159, 111020-111020 [10.1016/j.postharvbio.2019.111020].

Availability:

This version is available at: <https://hdl.handle.net/11585/713466> since: 2020-01-14

Published:

DOI: <http://doi.org/10.1016/j.postharvbio.2019.111020>

Terms of use:

Some rights reserved. The terms and conditions for the reuse of this version of the manuscript are specified in the publishing policy. For all terms of use and more information see the publisher's website.

This item was downloaded from IRIS Università di Bologna (<https://cris.unibo.it/>).
When citing, please refer to the published version.

(Article begins on next page)

I don't believe they have been able to show that any specific cultivar is better for fresh cut treatment based on their data.

Mendoza-Enano, M. L., Stanley, R., & Frank, D. (2019). Linking consumer sensory acceptability to volatile composition for improved shelf-life: A case study of fresh-cut watermelon (*Citrullus lanatus*). *Postharvest Biology and Technology*, *154*, 137-147.

Highlights

- Nectarine volatilome investigation by chromatographic and direct injection analysis.
- Fresh-cut processing modifies the VOC profile of nectarine
- Fresh-cut nectarines emit off-flavours without any visual deterioration symptoms.
- Development of a VOC biomarkers array to predict fresh-cut nectarine storability.

1 **Nectarine volatilome response to fresh-cutting and storage**

2

3 Ceccarelli A.^{1#}, Farneti B.^{2* #}, Khomenko I.², Cellini A.¹, Donati I.¹, Aprea E.², Biasioli F.², Spinelli

4 F.¹

5

6 ¹ Department of Agricultural and Food Sciences, Alma Mater Studiorum - University of Bologna,
7 viale G. Fanin 44, 40127 Bologna, Italy.

8

9 ²Research and Innovation Centre, Fondazione Edmund Mach, via Mach 1, 38010 San Michele all’
10 Adige, Trento, Italy.

11

12 #Equal contribution

13 *Author for correspondence: Farneti Brian (brian.farneti@fmach.it)

14

15 **Keywords:** VOCs; *Prunus persica*; minimal processing; cold storage; PTR-ToF-MS; SPME/GC-

16 MS

17

18

19

20

21

22

23

24

25

26

27 **Abstract**

28 The offer of fresh-cut peaches and nectarines represents a valid alternative for stone fruit
29 commercialization and matches the increasing market demand of ready-to-eat (RTE) products.

30 In this study we explored the effect of fruit processing and storage on the volatilome of RTE
31 fresh-cut nectarine. Fruit of three cultivars were sliced and packed in an industrial line and stored
32 for 5 d at 5 °C. Volatile organic compound (VOC) evolution was assessed **daily** in both intact and
33 processed fruit by an exhaustive untargeted analysis, performed by **proton transfer reaction-time of**
34 **flight-mass spectrometry (PTR-ToF-MS)** and **solid phase microextraction- gas chromatography-**
35 **mass spectrometry (SPME/GC-MS).**

36 Fresh-cut processing induced a major variation in nectarine volatilome depending on genetic
37 differences and storage. **This volatilome amelioration may be considered as an applicable strategy**
38 **to enhance peach and nectarine perceived quality.** Moreover, results of this study allowed the
39 detection of a set of possible biomarkers enabling the selection of the best nectarine genotypes for
40 processing and the prediction of the product shelf life based on the release of flavours and off-
41 flavours.

42

43 **1. Introduction**

44 The market supply of ready-to-eat (RTE) fresh-cut fruit has increased over the last years in
45 response to the rising demand of convenience and ready-to-use (RTE) products more aligned to the
46 modern life-style (Cavaiuolo et al., 2015; Denoya et al., 2017). **Thus, RTE fresh-cut stone fruit may**
47 **represent a valuable alternative to improve the marketability of peach and nectarine (Ceccarelli,**
48 **2018), which consumption has decreased over the last decades, mostly due to the poor flavour**
49 **characteristics perceived by consumers (Belisle et al., 2017; Cantin et al., 2009).** However,

50 achieving high quality fresh-cut peaches and nectarines still represents a technological challenge for
51 the industry.

52 Fresh-cut processing consists of two main mechanical operations, slicing and coring, that are
53 critical to determine the potential shelf life of the fresh-cut product (Soliva-Fortuny & Martín-
54 Belloso, 2003). These operations induce the disruption of the cell compartmentalization releasing
55 lytic enzymes and metabolites that trigger tissue degradation. Furthermore, wound stress, caused by
56 cutting and slicing, may accelerate the progression of fruit maturity and senescence, enhanced by an
57 increase of ethylene emission (Varoquaux & Wiley, 2017). The increased fruit perishability, flesh
58 softening and surface browning are the main negative consequences of fruit fresh-cutting (Artés &
59 Gómez, 2006) and the major impediment for the successful commercialization of RTE fresh-cut
60 fruit (Eissa et al., 2006). Unfortunately, in the fresh-cut industry, it is still generally assumed that “if
61 it looks good, it tastes good” (Beaulieu & Baldwin, 2002). Inconsistent or unsatisfactory aroma and
62 flavour quality may be one of the main reasons of the slow growth for fresh-cut fruit market
63 (Mendoza-Enano et al. 2019).

64 Aroma is considered a key component in determining peach consumer satisfaction (Wang et
65 al., 2009; Belisle et al., 2017). It relies on the complex interaction of several VOC classes, including
66 esters, C6 aldehydes, terpenes, alcohols, and lactones (Wang et al., 2009; Yang et al., 2009;
67 Eduardo et al., 2010). The latter molecular class is reported to include some of the major
68 contributors of the peach and nectarine aroma (Lavilla et al. 2002). Peach and nectarine aroma may
69 easily deteriorate during cold storage (Zhang et al., 2011; Cano-Salazar et al., 2013; Ceccarelli et
70 al., 2018) due to the insurgence of off-flavour compounds, mainly induced by chilling injury and
71 fermentative metabolism.

72 Several studies were performed to extend the shelf life of processed peaches and nectarines.
73 Most of these studies were focused on the processing suitability of different cultivars, (Giné
74 Bordonaba et al., 2014; Denoya et al., 2017), heat treatments (Koukounaras et al., 2008),

75 application of edible coatings (Pizato et al., 2013), inactivation of enzymatic activities by high
76 pressure processing (Denoya et al., 2015; Denoya et al., 2016), low temperature storage, and
77 modified atmosphere packaging (MAP) (Koukounaras et al., 2008). However, no thorough
78 investigation has been conducted so far on the development of the flavour and off-flavour
79 **generation** during processing and storage of RTE fresh-cut peaches. Packed fruit may easily ferment
80 when the O₂ level is below an optimal concentration (Solomos, 1994), thus inducing the synthesis
81 of ethanol, acetaldehyde, and acetic acid.

82 **Therefore, a thorough characterization of VOC emission evolution during storage and**
83 **ripening is important to monitor and predict the quality of RTE fresh-cut peaches and nectarines**
84 **(Ceccarelli, 2018).** To achieve these results, a deeper understanding of the influence of peach and
85 nectarine varieties, harvest conditions, maturity, storage and shelf life with regard to flavour
86 development is required (Colantuono et al., 2012).

87 In the present study, the volatilome of RTE fresh-cut nectarines was assessed **daily**, during
88 refrigerated storage, by an exhaustive untargeted VOC analysis, performed by two complementary
89 methods: PTR-ToF-MS (proton transfer reaction-time of flight-mass spectrometry) and SPME/GC-
90 MS (solid phase microextraction- gas chromatography-mass spectrometry). The aim was to explore
91 the effect of fruit processing (slicing, coring and packing) on VOC development during storage in
92 relation to cultivar differences and to determine a pool of putative volatile biomarkers useful to
93 predict the RTE fresh-cut product deterioration and its end-life.

94

95 **2. Material and methods**

96 **2.1 Plant material and fruit segregation into homogeneous group**

97 Nectarines (*Prunus persica*, L. Batch) from three cultivars, ‘Western Red’ (WR), ‘August
98 Red’ (AR) and ‘Morsiani 60’ (M60), were collected from a commercial packhouse located in
99 Faenza, Emilia Romagna, Italy.

100 Fruit of each cultivar was sorted into homogeneous batches, based on the fruit maturity stage,
101 to minimise fruit biological variability. Maturity was determined with the DA-Meter (TR, Forli,
102 Italy), a VIS-spectrometer that measures non-destructively the chlorophyll-a content in the fruit
103 flesh and peel (Farneti et al., 2015a). Maturity stages were expressed as Index of Absorbance
104 Difference (I_{AD}) ranging from 0.0 to 2.0 with the lower values indicating a more advanced fruit
105 maturity (Bonora et al., 2014). **In this study, only fully ripe nectarines (I_{AD} between 0.6 and 0.4)**
106 **were considered.**

107

108 **2.2 Experimental design**

109 **Sixty** nectarines per each cultivar were collected and sorted into two batches of **30** fruit each.
110 The first batch was fresh-cut processed, whilst the second was maintained intact. Both RTE fresh-
111 cut and intact nectarines were stored at 5 °C for 5 d to simulate the refrigerated storage. Five
112 biological replicates for both intact and fresh-cut fruit were daily analysed to assess quality traits
113 and VOC emission by PTR-ToF-MS. For each cultivar, SPME/GC-MS analysis was carried out on
114 a pooled sample at day 0, 2 and 4 to validate and support **the identification of compounds** in PTR-
115 ToF-MS analysis.

116 Nectarines were processed in an industrial line commercially used to produce fresh-cut pome
117 and stone fruit (Macè s.r.l., Ferrara, Italy) according to commercial standards. Prior to fresh-cut
118 processing, each fruit was washed and dipped for 2 min in a solution of water and peracetic acid to
119 eliminate skin contaminants. Slicing was performed by pushing the fruit longitudinally with a
120 pneumatic plunger through a sharp corer, producing eight symmetrical slices of homogeneous
121 thickness. Fruit core was automatically discarded whilst slices, transported by a conveyor belt, were
122 soaked for 1 min in an antioxidant solution (2.5 g L⁻¹ ascorbic acid, 2.5 g L⁻¹ sodium ascorbate) to
123 prevent surface browning. **Twenty slices, of approximately 10 g each, were automatically packed**

124 into commercial polypropylene boxes heat-welded with a micro-perforated (30 µm) plastic film.

125 Intact and fresh-cut fruit was then maintained at 5 °C until analysis.

126

127 **2.3 Surface browning and colour assessment**

128 Surface browning and flesh colour of nectarine wedges was evaluated with a Minolta CR-400
129 chromameter (Konica Minolta, Tokyo, Japan), using the L*a*b* parameters under the CIE standard
130 illuminant D65 (Caceres et al., 2016). At each assessment, intact fruit were sliced, and fruit flesh
131 colour was immediately measured to evaluate the colour evolution during fridge conservation.
132 Chroma was derived from the above-mentioned chromatic parameters. Surface browning was
133 estimated as browning index (BI), a parameter closely related to PPO (Polyphenol oxidase) activity
134 (Denoya et al., 2017) and calculated as following (Mohammad et al., 2008):

135 eq.1: $BI = 100 \times \frac{(x - 0.31)}{0.172}$ where $x = \frac{(a + 1.75L)}{(5.654L + a - 3.012b)}$

136

137 **2.4 Sample preparation for VOC analysis**

138 Intact and fresh-cut nectarines, including the skin, were immediately frozen in liquid nitrogen
139 and ground with a stainless-steel analytical mill (IKA, Staufen, Germany). For both PTR-ToF-MS
140 and SPME/GC-MS analysis 1 g of powdered frozen fruit was transferred into a 20-mL glass vial
141 sealed with 18 mm PTFE/silicon septa (Agilent Technologies, Santa Clara, USA). 1 mL of
142 antioxidant solution (400 g L⁻¹ of sodium chloride, 5 g L⁻¹ of ascorbic acid, and 5 g L⁻¹ of citric
143 acid) was added to each vial to prevent tissue oxidation (Farneti et al., 2014). Samples were kept at
144 -80 °C before being analysed.

145

146 **2.5 VOC analysis by PTR-ToF-MS**

147 Direct injection VOC measurement of nectarine tissue was performed in five replicates with a
148 commercial PTR-ToF-MS 8000 apparatus (Ionicon Analytik GmbH, Innsbruck, Austria) according

149 to the set-up described by Farneti et al., 2014. The drift tube conditions were the following: 110 °C
150 drift tube temperature, 2.30 mbar drift pressure, 550 V drift voltage. This leads to an E/N ratio of
151 about 140 Townsend (Td) (E corresponding to the electric field strength and N to the gas number
152 density; $1 \text{ Td} = 10^{-17} \text{ V cm}^2$). The sampling time per channel of ToF acquisition was 0.1 ns,
153 amounting to 350,000 channels for a mass spectrum ranging up to $m/z = 400$. Every single spectrum
154 is the sum of about 28.600 acquisitions lasting 35 μs each, resulting in a time resolution of 1 s.
155 Sample measurements were performed in 60 cycles resulting in an analysis time of 60 s/sample.

156 Each measurement was conducted automatically after 20 min of sample incubation at 40 °C
157 by using an adapted GC autosampler (MPS Multipurpose Sampler, GERSTEL) and it lasted for 2
158 min (Capozzi et al., 2017).

159 The analysis of PTR-ToF-MS spectral data proceeded as follows. Count losses due to the ion
160 detector dead time were corrected off-line via a methodology based on Poisson statistics. To reach a
161 good mass accuracy (up to 0.001 Th), internal calibration was performed according to a procedure
162 described by Cappellin et al. (2011a). Noise reduction, baseline removal and peak intensity
163 extraction were performed according to Cappellin et al. (2011b), using modified Gaussian
164 distributions to fit the peaks. Absolute headspace VOC concentrations expressed in $\mu\text{g Kg}^{-1}$
165 headspace for intact and processed fruit, were statistically analysed according to ANOVA and
166 **Tukey's Honestly Significant Difference (HSD) test ($P < 0.05$) when necessary.**

167

168 **2.6 VOC analysis by SPME/GC-MS**

169 Vials, containing the powdered sample and the antioxidant solution, were equilibrated at
170 40 °C for 10 min with constant stirring. A 2 cm solid-phase microextraction fibre
171 (DVB/CAR/PDMS, Supelco, Bellefonte, USA) was exposed for 30 min to the vial headspace. The
172 trapped compounds by SPME were analysed with a GC interfaced with a mass detector operating in
173 electron ionization (EI) mode (internal ionization source; 70 eV) with a scan range of m/z 33 to 350

174 (GC Clarus 500, PerkinElmer, Norwalk, USA). Separation was carried out in an HP-INNOWax
175 fused silica capillary column (30 m, 0.32-mm ID, 0.5- μ m film thickness; Agilent Technologies,
176 Santa Clara, USA). The initial GC oven temperature was 40 °C rising to 220 °C at 4 °C min⁻¹, the
177 temperature of 220 °C was maintained for 1 min, then increased at 10 °C min⁻¹ until it reached
178 250 °C, which was maintained for 1 min. The carrier gas was helium at a constant column flow rate
179 of 1.5 mL min⁻¹. Semi-quantitative data were expressed as area units. Compounds identification was
180 based on mass spectra matching with the standard NIST/EPA/NIH (NIST 14) and Wiley 7th Mass
181 Spectral Libraries, and linear retention indices (LRI) compared with the literature. LRI were
182 calculated under the same chromatographic conditions after injection of a C7–C30 n-alkane series
183 (Supelco, Bellafonte, USA).

184

185 **2.7 Data analysis**

186 The array of masses detected by PTR-ToF-MS was reduced by applying noise and correlation
187 coefficient thresholds. In the first case, peaks not significantly different from blank samples were
188 removed (Farneti et al., 2015b). Regarding correlation coefficient thresholds, peaks having over
189 99 % correlation were excluded as putative isotopes of monoisotopic masses (Farneti et al., 2017).

190 Data analysis was performed with R.3.3.3 software using internal functions and the external
191 packages “mixOmics” and “heatmap3” for multivariate statistical analysis (PCA and hierarchical
192 clustering), “Agricolae” for ANOVA and post hoc comparisons, and “ggplot2” for graphic
193 representations. Multivariate statistical analysis was performed on log transformed and centred data.
194 The estimation of the optimal number of clusters was computed by performing silhouette and gap
195 statistics.

196

197 **3. Results and discussion**

198 **3.1 Untargeted nectarine volatilome assessment**

199 The characterisation of nectarine volatilome by gas chromatographic and direct injection mass
200 spectrometric analysis allowed the detection of all the main VOCs responsible for nectarine aroma
201 (Tab. 1 and Tab. 2), reported in recent literature both with HS-SPME/GC-MS (Brizzolara et al.,
202 2018) and PTR-ToF-MS (Bianchi et al., 2017) analysis.

203 The headspace VOC analysis of both intact and fresh-cut fruit, assessed in the three nectarine
204 cultivars, allowed the detection of 73 compounds (Tab. 1), only one of which was not identified.
205 Alcohols are the most representative VOC class in terms of number of compounds (14), followed
206 by esters (13), aldehydes (10), monoterpenes (10), acids (7), lactones (6), ketones (5), hydrocarbons
207 (2), methylphenols (2), norisoprenoids (1) and sesquiterpenes (1). Concerning VOC relative
208 concentration (STab. 1), aldehydes (primarily hexanal, pentenal, and (E)-2-hexenal) were the most
209 representative class in intact nectarine fruit, representing 50.6 % of total VOC profile of WR,
210 69.9 % for AR, and 92.2 % for M60. Monoterpenes, for the most linalool, were the second
211 representative group accounting for 21.2 % of the total VOC content of WR, 2.5 % for AR and
212 1.6 % for M60. Esters (for the most hexyl acetate, isoamyl acetate and butyl acetate) were mostly
213 representative in AR, accounting for 9.9 % of the total volatiles and 5.5 % in WR. For M60 the total
214 ester concentration was only 0.9 % of the total VOCs. Alcohols (mostly 1-pentanol) accounted for
215 about 7.2 % of the total VOC profile of AR and 7.7 % for WR whilst only 1.6 % for M60. The
216 highest fraction of lactones was composed by γ -hexalactone and γ -decalactone and represented
217 4.7 % of the VOC profile of WR, 1.2 % for AR and 1 % for M60. Ketones concentration (for the
218 most 1-octen-3-one and 6-methyl-5-hepten-2-one) represented 3.3 % of the WR volatiles, 2.8 % of
219 AR and 0.8 % of M60. Sesquiterpenes, represented only by nerolidol, were mostly detected in WR,
220 accounting for 1.8 % of the cultivar's VOC profile, while this class only amounted to 0.03 % in AR
221 and it was not detected in M60. Hydrocarbons such as toluene and styrene accounted for 1.9 % of
222 the total volatiles of AR, 1.3 % for WR and 0.45 % for M60. Acids (for the most isovaleric acid and
223 pentanoic acid) accounted for 0.9 % of the VOC profile for WR and AR whilst 0.36 % for M60. β -

224 damascenone (norisoprenoids) accounted for 0.1 % of the VOC profile in WR, 0.04 % in AR, and
 225 0.03 % in M60.

226

227

228 **Table 1.** Volatile compounds detected by SPME/GC-MS immediately after harvest. Values are
 229 reported as percentage of total peak area per chromatogram.

	ID	Formula	KI Calc	KI NIST	Western Red		August Red		Morsiani 60	
					Intact	Processed	Intact	Processed	Intact	Processed
ACIDS										
Acetic Acid	Ac_1	C ₂ H ₄ O ₂	1562	1449	0.11	0	0.19	0.02	0.05	0.07
Isovaleric Acid	Ac_2	C ₅ H ₁₀ O ₂	1748	1666	0.23	0.23	0.25	0.12	0.16	0.25
Butanoic Acid	Ac_3	C ₄ H ₈ O ₂	1821	1625	0.07	0.05	0.04	0.01	0.01	0.01
Pentanoic Acid	Ac_4	C ₅ H ₁₀ O ₂	1922	1733	0.3	0.29	0.2	0.07	0.1	0.12
2-Ethyl Hexanoic Acid	Ac_5	C ₈ H ₁₆ O ₂	2003	1960	0	0	0.01	0	0	0
Hexanoic Acid	Ac_6	C ₆ H ₁₂ O ₂	2025	1846	0.09	0.05	0.07	0.02	0.02	0.02
Heptanoic Acid	Ac_7	C ₇ H ₁₄ O ₂	2198	1950	0.09	0.04	0.11	0.02	0.02	0.02
Total (%)					0.89	0.66	0.87	0.26	0.36	0.49
ALCOHOLS										
3-Pentanol	Al_1	C ₅ H ₁₂ O	1125	1110	0.18	0.09	0.19	0.01	0.04	0.03
1-Butanol	Al_2	C ₄ H ₉ OH	1162	1142	0.23	0.09	0.04	0.01	0.02	0.02
2+3-Methyl-1-Butanol	Al_3	C ₅ H ₁₂ O	1225	1208+1209	0.12	0.27	0.09	0.05	0.06	0.12
1-Pentanol	Al_4	C ₅ H ₁₂ O	1266	1250	2.59	2.04	1.43	0.28	0.36	0.17
Hexanol	Al_5	C ₆ H ₁₄ O	1366	1355	0.41	0.46	0.43	0.19	0.11	0.34
3-Octanol	Al_6	C ₈ H ₁₈ O	1404	1393	0	0.29	0.01	0	0	0
(Z)-2-Hexen-1-ol	Al_7	C ₆ H ₁₂ O	1417	1416	0.04	0.19	0.06	0.16	0.04	0.08
1-Octen-3-ol	Al_8	C ₈ H ₁₆ O	1460	1450	0.57	0.39	0.41	0.12	0.18	0.11
1-(2-Methoxy-1-methylethoxy)-2-propanol	Al_9	C ₇ H ₁₆ O ₃	1486	1478	0.05	0.05	0.43	0	0.02	0.05
2-Ethyl-1-Hexanol	Al_10	C ₈ H ₁₈ O	1497	1491	0.34	0.49	0.49	0.24	0.09	0.2
1-(2-methoxypropoxy)-2-propanol	Al_11	C ₇ H ₁₆ O ₃	1526	1532	0.31	0.21	1.5	0.1	0.09	0.2
1-Octanol	Al_12	C ₈ H ₁₈ O	1565	1557	0.37	0.43	0.34	0.2	0.15	0.08
2-phenyl isopropanol	Al_13	C ₉ H ₁₂ O	1763	1773	0.49	0.32	0.55	0.11	0.14	0.09
Phenol	Al_14	C ₆ H ₆ O	2010	2000	0.5	0.33	0.5	0.09	0.12	0.09
Total (%)					6.2	5.65	6.47	1.56	1.42	1.58
ALDEHYDES										
Butanal	Ad_1	C ₄ H ₈ O	902	877	0.52	2.26	0.33	0.14	0.12	0.35
Pentanal	Ad_2	C ₅ H ₁₀ O	980	979	11.83	6.99	8.89	1.13	2	0.81
Hexanal	Ad_3	C ₆ H ₁₂ O	1094	1083	18.33	7.11	22.78	6.98	28.14	29.42
(2E)-Hexenal	Ad_4	C ₆ H ₁₀ O	1230	1216	5.63	9.8	29.48	19.29	55.62	49.93
Octanal	Ad_5	C ₈ H ₁₆ O	1300	1289	2.69	1.82	1.82	0.35	1.48	0.41
2-Heptenal	Ad_6	C ₇ H ₁₂ O	1330	1323	4.13	2.38	2.57	0.28	1.09	0.59
Nonanal	Ad_7	C ₉ H ₁₈ O	1399	1391	3.59	2.24	1.37	0.34	2.02	0.66
(E)-2-Octenal	Ad_8	C ₈ H ₁₄ O	1432	1429	2.73	1.44	1.73	0.42	0.76	0.36
Decanal	Ad_9	C ₁₀ H ₂₀ O	1500	1498	0.73	0.71	0.36	0.13	0.76	0.24

Benzaldehyde	Ad_10	C ₇ H ₆ O	1522	1520	0.42	0.3	0.6	0.28	0.25	0.49
Total (%)					50.6	35.05	69.93	29.34	92.24	83.26
ESTERS										
Ethyl Acetate	E_1	C ₄ H ₈ O ₂	893	888	0.22	4.53	0.38	0.19	0.13	0.81
Isobutyl Acetate	E_2	C ₆ H ₁₂ O ₂	1019	1012	0.15	2.55	0.16	0.25	0.08	0.35
Butyl Acetate	E_3	C ₆ H ₁₂ O ₂	1084	1074	1.07	1.98	2.22	0.28	0.19	0.46
Isoamyl Acetate + Ethyl Benzene	E_4		1135	1122+1129	1.36	0.74	2.29	0.21	0.25	0.33
Ethyl Crotonate	E_5	C ₆ H ₁₀ O ₂	1179	1160	0	0	0.01	0.25	0	0
Amyl Acetate	E_6	C ₇ H ₁₄ O ₂	1190	1176	0.08	0.99	0.15	0.05	0	0.11
Ethyl Hexanoate	E_7	C ₈ H ₁₆ O ₂	1247	1233	0	0.07	0.01	0.53	0	0
Hexyl Acetate	E_8	C ₈ H ₁₆ O ₂	1286	1272	2.26	4.02	4.22	2.6	0.23	4.23
(Z)-3-Hexenyl Acetate	E_9	C ₈ H ₁₄ O ₂	1329	1315	0.14	3.36	0.21	2.79	0.02	0.32
(E)-2-Hexenyl Acetate	E_10	C ₈ H ₁₄ O ₂	1346	1333	0	2.55	0.09	2.74	0	0.39
Hexyl Butanoate	E_11	C ₁₀ H ₂₀ O ₂	1421	1414	0.05	0.01	0.1	0.02	0	0
Ethyl Octanoate	E_12	C ₁₀ H ₂₀ O ₂	1441	1435	0	0.65	0.01	0.07	0	0.21
Benzyl Acetate	E_13	C ₉ H ₁₀ O ₂	1731	1720	0.16	0.15	0.13	0.02	0	0
Total (%)					5.49	21.6	9.98	10	0.9	7.21
HYDROCARBONS										
Toluene	H_1	C ₇ H ₈	1045	1042	0.95	0.56	1.29	0.43	0.26	0.34
Styrene	H_2	C ₈ H ₈	1269	1261	0.37	0.17	0.59	0.21	0.2	0.29
Total (%)					1.32	0.73	1.88	0.64	0.46	0.63
ISOTHIOCYANATES										
Isothiocyanato Cyclohexane	I_1	C ₇ H ₁₁ NS	1661	1667	1.83	1.14	2.53	0.47	0.66	0.43
Total (%)					1.83	1.14	2.53	0.47	0.66	0.43
KETONES										
Acetoin	K_1	C ₄ H ₈ O ₂	1295	1284	0	0.08	0.01	0.01	0	0.02
1-octen-3-one	K_2	C ₈ H ₁₄ O	1312	1300	1.15	0.71	0.67	0.16	0.35	0.15
2,5-Octanedione	K_3	C ₈ H ₁₄ O ₂	1339	1319	0.95	0.63	0.81	0.15	0.24	0.12
6-Methyl-5-Hepten-2-one	K_4	C ₈ H ₁₄ O	1347	1338	1.06	0	1.26	0	0.22	0.08
2-Undecanone	K_5	C ₁₁ H ₂₂ O	1598	1598	0	0.11	0.01	0.01	0	0.02
Total (%)					3.16	1.53	2.76	0.33	0.81	0.39
LACTONES										
γ-Hexalactone	L_1	C ₆ H ₁₀ O ₂	1696	1694	3.5	4.59	0.69	0.39	0.93	0.69
γ-Octalactone	L_2	C ₈ H ₁₄ O ₂	1907	1910	0.09	0.09	0.01	0.01	0	0.02
γ-Decalactone	L_3	C ₁₀ H ₁₈ O ₂	2112	2138	0.63	0.64	0.31	0.12	0.06	0.09
6-pentyl-2H-Pyran-2-one	L_4	C ₁₀ H ₁₄ O ₂	2139	2171	0.16	0.18	0.05	0.02	0	0
δ-Decalactone	L_5	C ₁₀ H ₁₈ O ₂	2151	2194	0.13	0.16	0.07	0.03	0.01	0.02
γ-Undecalactone	L_6	C ₁₁ H ₂₀ O ₂	2300	2259	0.33	0.19	0.11	0.03	0.01	0.01
Total (%)					4.84	5.85	1.24	0.6	1.01	0.83
METHYLPHENOLS										
4-Methyl Phenol	Mp_1	C ₇ H ₈ O	2073	2080	0.18	0.11	0.17	0.03	0.04	0.04
3-Methyl Phenol	Mp_2	C ₇ H ₈ O	2079	2091	0.73	0.53	0.77	0.14	0.22	0.17
Total (%)					0.91	0.64	0.94	0.17	0.26	0.21
MONOTERPENES										
β-Myrcene	Mt_1	C ₁₀ H ₁₆	1175	1161	0.06	0.07	0.01	0.35	0	0.03
Limonene	Mt_2	C ₁₀ H ₁₆	1206	1199	0.17	12.67	1.08	52.71	0.26	4.11
Linalool	Mt_3	C ₁₀ H ₁₈ O	1555	1547	20.65	11.05	0.99	3.06	1.21	0.73
4-Terpineol	Mt_4	C ₁₀ H ₁₈ O	1601	1602	0	0.04	0.01	0.07	0	0.01
HO Trienol	Mt_5	C ₁₀ H ₁₆ O	1616	1613	1.38	1.31	0.71	0.19	0.17	0.09

Carvone	Mt_6	C ₁₀ H ₁₄ O	1727	1740	0	0.12	0.01	0.04	0	0.02
Epoxylinalool	Mt_7	C ₁₀ H ₁₈ O ₂	1767	1721	0.05	0.1	0.02	0.04	0.01	0.01
trans-Carveol	Mt_8	C ₁₀ H ₁₆ O	1836	1845	0	0	0.01	0.02	0	0
Geraniol	Mt_9	C ₁₀ H ₁₈ O	1852	1847	0.31	0.26	0.33	0.09	0.08	0.07
2,6-dimethyl-3,7-octadiene-2,6-diol	Mt_10	C ₁₀ H ₁₈ O ₂	1953	1945	0.1	0.05	0.04	0.02	0.01	0
Total (%)					22.72	25.67	3.21	56.59	1.74	5.07
NORISOPRENOIDS										
β-Damascenone	N_1	C ₁₃ H ₁₈ O	1814	1823	0.1	0.03	0.04	0.01	0.03	0.02
Total (%)					0.1	0.03	0.04	0.01	0.03	0.02
SESQUITERPENES										
Nerolidol	S_1	C ₁₅ H ₂₆ O	2035	2034	1.83	1.48	0.03	0.01	0	0
Total (%)					1.83	1.48	0.03	0.01	0	0
UNKNOWN										
Unknown	U_1	Unknown	1429	1432	0.09	0	0.18	0	0	0
Total Area	(x 10⁶)				245.1	359.6	182.9	987.18	583.4	836.8

230

231

232 The PTR-ToF-MS setting adopted in this study allowed the detection of the full VOC spectra
 233 in 1 s. Only the first 30 s of the full measurement (60 s) were analysed and averaged, to avoid
 234 possible measurement inaccuracies caused by an excessive dilution of the sample headspace. The
 235 whole VOC spectra, assessed in five biological replicates per sample, were reduced from 223 to 112
 236 masses, applying noise, and correlation coefficient thresholds. The exact chemical molecular
 237 formula was identified for 90 detected masses, while a more precise tentative identification, based
 238 on literature references, chemical standards, and correlation with SPME/GC-MS analysis, was
 239 possible for 68 masses (Tab. 2).

240 VOC screening by PTR-ToF-MS allowed the detection of additional compounds not detected
 241 by SPME/GC-MS analysis. Among the most representative, ethanol (*m/z* 47.049) and methanol
 242 (*m/z* 33.033) represented the highest fraction of the detected alcohols, whilst among the aldehydes,
 243 acetaldehyde (*m/z* 45.032) was the most represented in the three cultivars. Ketones, such as acetone
 244 (*m/z* 59.049), and sulfur compounds, tentatively identified as hydrogen sulfide (*m/z* 34.995),
 245 methanethiol (*m/z* 49.010) and dimethyl sulfide and/or ethanethiol (*m/z* 63.029), were also detected
 246 in the three nectarine cultivars.

247

248

249

250

251 **Table 2.** Volatile organic compounds detected by PTR-ToF-MS **immediately after harvest**. Values are
 252 reported as concentration ($\mu\text{g Kg}^{-1}$). * indicates compounds identified by SPME/GC-MS and [a]
 253 indicates compounds identified by Bianchi et al., 2017. **For each compound, values with the same**
 254 **letter are no significantly different between cultivars and intact and processed fruit according to**
 255 **ANOVA and Tukey HSD ($P < 0.05$).**

256

m/z	Formula	Tentative identification	<i>Western Red</i>		<i>August Red</i>		<i>Morsiani 60</i>	
			Intact	Processed	Intact	Processed	Intact	Processed
27.026	C2H3+	Common fragment	0.21 bc	0.43 ab	0.17 bc	0.41 ab	0.08 c	0.62 a
27.034		n.i.	0.03 cd	0.19 bc	0.07 bcd	0.23 ab	0.03 d	0.39 a
27.043		n.i.	0.05 b	0.09 ab	0.05 b	0.12 ab	0.02 b	0.17 a
28.018	C [13]CH3+	n.i.	0.38 a	0.35 a	0.52 a	0.62 a	0.32 a	0.46 a
28.031	C2H4+	Ethylene	0.15 b	0.30 ab	0.26 ab	0.38 a	0.12 b	0.37 a
29.039	C2H5+	Ethanol fragment	3.74 c	50.30 ab	1.72 c	36.99 b	2.38 c	79.78 a
31.018	CH2OH+	Formaldehyde	3.39 bc	5.02 ab	3.15 bc	4.87 b	2.27 c	6.82 a
33.033	CH4OH+	Methanol	207.91 bc	375.24 ab	255.99 bc	326.32 ab	98.86 c	465.21 a
34.995	H2SH+	Hydrogen sulfide	5.37 a	3.51 a	3.57 a	5.56 a	2.90 a	5.27 a
39.022	C3H3+	Common fragment	9.97 ab	8.19 ab	6.94 b	6.67 b	3.49 b	15.30 a
41.038	C3H5+	Common fragment	36.29 a	32.65 ab	26.70 ab	32.93 ab	11.04 b	44.81 a
42.010	C2H2O+	n.i.	0.10 bc	0.25 ab	0.14 bc	0.25 ab	0.07 c	0.36 a
42.033	C2H3NH+	Acetonitrile	0.72 a	1.24 a	1.24 a	1.25 a	0.70 a	1.42 a
43.017	C [13]CH3O+	Common fragment	37.29 c	216.18 a	39.36 bc	82.36 bc	19.56 c	167.93 ab
43.054	C2[13]CH7+	Common fragment	8.13 ab	10.47 ab	9.68 ab	15.66 a	3.48 b	12.55 a
45.032	C [13]CH4OH+	Acetaldehyde	94.46 c	993.58 b	163.24 c	1447.46 b	47.42 c	2276.30 a
47.049	C [13]CH6OH+	Ethanol	19.47 c	231.60 ab	6.20 c	197.10 b	10.21 c	381.13 a
49.010	CH4SH+	Methanethiol	0.90 a	0.37 b	0.67 ab	1.03 a	0.37 b	0.54 ab
51.022		n.i.	0.32 a	0.41 a	0.20 a	0.24 a	0.17 a	0.52 a
53.038	C4H5+	n.i.	1.87 ab	1.49 ab	1.82 ab	1.76 ab	1.03 b	3.78 a
55.016		n.i.	0.07 a	0.34 a	0.23 a	0.17 a	0.08 a	0.35 a
55.054	C4H7+	Common fragment	47.47 ab	33.05 ab	50.07 ab	52.88 ab	16.43 b	94.95 a
57.033	C3H4OH+	Common fragment	13.17 ab	9.01 b	35.79 ab	17.69 ab	19.83 ab	66.73 a
57.070	C4H9+	1-Butanol*, high alcohol fragment	11.80 ab	29.52 a	5.65 b	14.64 ab	2.32 b	16.99 ab
59.049	C3H6OH+	Acetone, propanal	61.98 a	82.16 a	72.26 a	84.73 a	40.46 a	85.12 a
60.021	C2H4O2+	n.i.	0.02 bc	0.11 a	0.02 bc	0.05 abc	0.01 c	0.09 ab
61.028	C [13]CH4O2H+	Acetic acid, fragment of Acetate esters*, Acetoin*	28.73 b	320.96 a	27.95 b	80.04 b	18.84 b	182.42 ab
63.008		n.i.	0.69 a	0.56 a	1.78 a	5.85 a	0.25 a	0.72 a
63.029	C2H6SH+	Dimethyl sulfide, ethanethiol	0.69 c	5.98 bc	1.26 c	11.87 a	0.31 c	11.67 ab
65.019		n.i.	2.90 abc	2.40 abc	3.84 ab	4.28 a	0.87 c	1.52 bc
65.057	C5H5+	Ethanol cluster	0.42 b	5.84 a	0.21 b	7.39 a	0.19 b	9.63 a
66.024		n.i.	0.06 ab	0.08 ab	0.11 ab	0.12 a	0.03 b	0.04 ab
67.054	C5H7+	n.i.	1.85 bc	1.34 bc	1.96 bc	4.62 a	0.60 c	2.50 b
68.058	C4[13]CH7+	n.i.	0.17 bc	0.13 bc	0.18 bc	0.48 a	0.06 c	0.21 b
69.033	C4H4OH+	Furan	0.60 ab	0.49 ab	0.57 ab	0.70 a	0.27 b	0.62 ab
69.070	C5H9+	Aldehyde fragment, isoprene	28.61 a	17.02 ab	20.31 ab	23.26 ab	7.32 b	32.90 a
70.041		n.i.	0.05 ab	0.11 a	0.08 ab	0.07 ab	0.03 b	0.10 a
71.049	C4H6OH+	Butenal, butenone	2.67 a	1.63 ab	2.20 a	2.53 a	0.69 b	2.16 a

71.085	C5H11+	3-methyl-1-butanol + 2-methyl-1-butanol*, 3-Pentanol*, 1-Pentanol*	2.57 ab	3.43 a	1.67 ab	2.60 ab	0.64 b	3.96 a
73.028	C3H4O2H+	n.i.	1.68 bc	1.55 cd	2.48 ab	3.01 a	0.79 d	1.65 c
73.065	C4H8OH+	Butanal*, 2-methylpropanal	12.94 c	109.16 a	7.69 c	43.44 bc	5.90 c	78.20 ab
75.044	C3H6O2H+	Methyl Acetate*, propanoic acid, propanoate ester fragment	8.80 ab	19.11 a	4.45 b	8.82 ab	2.13 b	12.75 ab
75.079	C4H10OH+	2-Methylpropanol [a], butanol	0.05 b	0.22 a	0.02 b	0.09 ab	0.03 b	0.21 a
77.019		n.i.	0.16 a	0.20 a	0.19 a	0.19 a	0.14 a	0.21 a
77.048		n.i.	0.23 a	0.28 a	0.19 a	0.25 a	0.16 a	0.26 a
77.072		n.i.	0.21 a	0.21 a	0.22 a	0.24 a	0.20 a	0.26 a
79.036		Acetic acid cluster	0.02 b	1.39 a	0.04 b	0.49 ab	0.05 b	0.81 ab
79.054	C6H7+	Benzene	5.44 a	4.91 a	4.91 a	3.82 a	3.01 a	4.38 a
80.058			0.37 ab	0.36 ab	0.48 a	0.51 a	0.22 b	0.41 ab
80.990		n.i.	15.53 ab	13.00 ab	20.06 ab	23.97 a	4.32 b	7.53 ab
81.070	C6H9+	Fragment of aldehydes (Hexenals); fragment of terpenes (Linalool)	8.94 b	12.20 b	38.19 b	130.90 a	6.89 b	32.59 b
83.049	C5H6OH+	Methylfuran	1.46 a	1.02 ab	1.05 ab	1.03 ab	0.49 b	1.50 a
83.086	C6H11+	(E)-3-Hexen-1-ol, (Z)-3-Hexen-1-ol, (Z)-2-Hexen-1-ol*, Hexanal, 2-Hexanone	36.01 ab	21.06 ab	38.75 ab	42.12 ab	12.04 b	72.63 a
84.053	C4[13]CH6OH+	n.i.	0.14 ab	0.10 ab	0.13 ab	0.13 ab	0.06 b	0.17 a
85.065	C5H8OH+	2-Pentenal [a]	4.76 a	2.19 a	4.02 a	4.23 a	1.63 a	4.91 a
87.044	C4H6O2H+	Butyrolactone	1.57 ab	1.51 ab	1.48 ab	1.94 a	0.59 b	1.54 ab
87.080	C5H10OH+	2-methyl butanal+3-methyl butanal, Pentanal*	5.06 ab	3.65 ab	3.99 ab	5.22 a	2.04 b	6.51 a
88.079		n.i.	0.51 a	0.60 a	0.89 a	0.99 a	0.52 a	0.96 a
89.059	C3[13]CH8O2H+	Ethyl Acetate*, Butanoic Acid*	2.27 b	79.97 a	1.13 b	13.68 b	2.40 b	39.72 ab
91.068	C7H7+	Benzyl Alcohol	0.45 bc	1.12 a	0.64 abc	0.98 ab	0.27 c	1.05 ab
93.036	C3H8OSH+	n.i.	1.73 ab	1.63 ab	2.29 a	2.47 a	0.91 b	2.61 a
93.069	C7H9+	Toluene*, Monoterpene fragment	8.55 abc	13.49 ab	4.81 bc	16.60 a	2.21 c	15.41 a
93.088		n.i.	0.22 a	0.43 a	0.15 a	0.40 a	0.08 a	0.34 a
95.018		n.i.	0.51 ab	0.48 ab	0.67 a	0.72 a	0.28 b	0.71 a
95.086	C7H11+	2-Heptenal*, Monoterpene fragment	2.88 b	2.63 b	3.62 b	18.68 a	0.65 b	3.81 b
97.028	C5H4O2H+	Furfural	1.00 ab	0.85 ab	0.81 ab	0.94 ab	0.43 b	1.42 a
97.065	C6H8OH+	2,4-Hexadienal, 2-ethylfuran	0.82 ab	0.49 bc	1.08 a	1.00 ab	0.27 c	0.72 abc
97.102	C7H13+	Heptanal, fragment	1.27 a	0.78 b	0.91 ab	1.19 a	0.24 c	0.70 b
99.080	C6H10OH+	2-Hexenal*, (2E)-Hexenal	4.31 ab	2.94 b	14.73 ab	7.95 ab	6.63 ab	22.59 a
101.060	C5H8O2H+	2,3-Pentanedione	0.59 a	0.38 ab	0.56 a	0.61 a	0.22 b	0.52 a
101.096	C6H12OH+	Hexanal*	5.14 ab	2.77 ab	5.60 ab	5.22 ab	1.71 b	10.28 a
103.075	C5H10O2H+	Isovaleric Acid*, Pentanoic Acid*	0.43 bc	0.77 ab	0.47 abc	0.76 ab	0.17 c	0.90 a
105.050	C4H8O3H+	n.i.	0.02 a	0.02 a	0.03 a	0.05 a	0.02 a	0.02 a
105.071	C8H9+	Styrene*	0.39 ab	0.39 ab	0.45 ab	0.77 a	0.24 b	0.48 ab
107.080	C8H10H+	Ethyl Benzene, Xylene	3.57 a	3.33 a	7.31 a	6.09 a	1.11 a	3.02 a
109.069	C7H8OH+	4-Methyl Phenol*, 3-Methyl Phenol*	0.08 a	0.08 a	0.12 a	0.12 a	0.09 a	0.08 a
109.103	C8H13+	n.i.	1.86 a	1.21 ab	1.79 a	1.89 a	0.43 b	1.29 a
113.024		n.i.	0.19 c	0.18 c	0.27 ab	0.31 a	0.13 c	0.20 bc
113.060	C6H8O2H+	Sorbic acid	0.20 bc	0.16 cd	0.30 ab	0.36 a	0.09 d	0.20 bc
113.096	C7H12OH+	Heptenal	1.12 a	0.64 ab	0.61 ab	0.89 a	0.18 b	0.65 ab
115.076	C6H10O2H+	Ethyl Crotonate (Ethyl (2E) -2-butenolate) *, 5-Ethylidihydro-2(3H)-Furanone*	0.38 a	0.29 ab	0.29 ab	0.31 a	0.12 b	0.37 a
115.113	C7H14OH+	Γ-Hexalactone*, Heptanone, Heptanal	0.37 ab	0.25 b	0.28 b	0.47 a	0.07 c	0.22 bc
117.091	C6H12O2H+	Isobutyl Acetate*, Butyl Acetate*, Hexanoic Acid*, ethyl butanoate	0.41 bc	1.12 a	0.51 bc	0.94 ab	0.24 c	0.72 abc
119.087	C9H11+	n.i.	0.14 bc	0.16 abc	0.15 abc	0.24 a	0.11 c	0.22 ab
121.066	C8H8OH+	Benzeneacetaldehyde [a]	0.15 bc	0.15 bc	0.24 a	0.25 a	0.10 c	0.19 ab
121.103	C9H13+	n.i.	0.40 b	0.40 b	0.40 b	0.99 a	0.23 b	0.41 b
123.083	C8H10OH+	2-phenylethanol, ethylphenol	0.08 ab	0.05 bc	0.10 a	0.10 a	0.03 c	0.08 abc
123.119	C9H15+	Nonenal	0.31 ab	0.25 b	0.32 ab	0.37 a	0.12 c	0.27 ab
125.098	C8H12OH+	Fragment of nonanal	0.60 a	0.38 a	0.44 a	0.51 a	0.11 b	0.41 a
127.113	C8H14OH+	1-octen-3-one*, 6-Methyl-5-Hepten-2-one*, (E)-2-Octenal*	1.62 a	0.90 ab	1.10 a	1.28 a	0.25 b	1.05 a
129.091	C7H12O2H+	γ-Heptalactone [a]	0.15 ab	0.16 ab	0.22 a	0.25 a	0.09 b	0.20 a
129.1293	C8H16OH+	2-octanone, Octanal*, 1-Octen-3-ol*	0.51 a	0.39 ab	0.40 a	0.56 a	0.11 b	0.35 ab
131.107	C7H14O2H+	Isoamyl Acetate+Ethyl Benzene*, Amyl Acetate*, Heptanoic Acid*	0.20 c	0.31 bc	0.42 b	0.60 a	0.14 c	0.42 b
135.114	C10H15+	HO-Trienol*, trans-Carveol*	0.23 b	0.26 b	0.33 b	0.76 a	0.16 b	0.31 b
137.134	C10H17+	(Limonene*, β-Myrcene*, Linalool*, 4-Terpineol*, Geraniol*	1.56 b	5.27 b	10.01 b	80.04 a	0.92 b	9.59 b

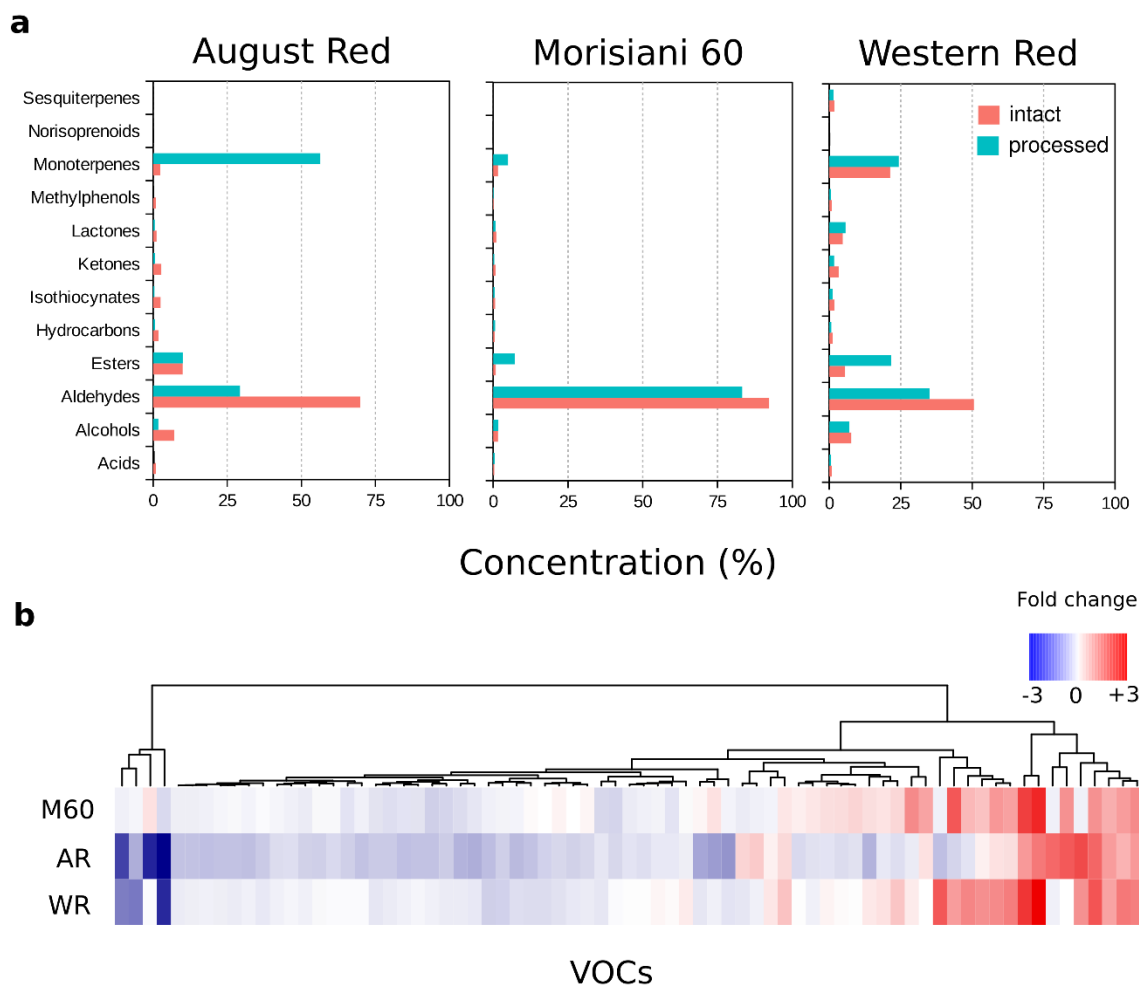
141.091	C8H13O2+	n.i.	0.05 c	0.05 c	0.11 ab	0.12 a	0.02 c	0.06 bc
141.129	C9H16OH+	2-Nonenal [a]	0.16 ab	0.14 bc	0.18 ab	0.20 a	0.07 c	0.17 ab
143.109	C8H14O2H+	cis-3-Hexenyl Acetate*, 2,5-Octanedione*, trans-2-Hexenyl Acetate*, 5-Butyldihydro-2(3H)-Furanone*	0.41 bc	0.39 bc	0.47 b	0.81 a	0.14 c	0.40 bc
145.124	C8H16O2H+	Ethyl Hexanoate*, Hexyl Acetate*, 2-Ethyl Hexanoic Acid*	0.15 c	0.29 c	0.32 bc	0.61 a	0.14 c	0.48 ab
149.051		n.i.	0.39 a	0.32 a	0.36 a	0.47 a	0.24 a	0.32 a
149.132	C11H17+	n.i.	0.03 b	0.05 ab	0.06 a	0.06 ab	0.04 ab	0.06 ab
153.130	C10H16OH+	HO-Trienol*, Epoxylinolool*, 2,4-Decadienal, 2,6-dimethyl-3,7-octadiene-2,6-diol*	0.14 bc	0.13 bc	0.16 abc	0.23 a	0.08 c	0.17 ab
155.103	C9H14O2H+	n.i.	0.30 b	0.31 b	0.61 a	0.66 a	0.19 c	0.28 bc
155.145	C10H18OH+	Linalool*, 4-Terpineol*	0.10 abc	0.08 bc	0.19 ab	0.20 a	0.06 c	0.13 abc
157.124	C9H16O2H+	n.i.	0.14 bc	0.14 bc	0.25 a	0.27 a	0.07 c	0.17 b
159.141	C9H18O2H+	methyl octanoate	0.22 c	0.22 c	0.37 ab	0.40 a	0.22 c	0.29 bc
163.097		n.i.	0.13 ab	0.09 ab	0.13 ab	0.20 a	0.05 b	0.09 ab
163.152	C12H19+	n.i.	0.01 b	0.02 ab	0.03 ab	0.04 a	0.02 b	0.02 ab
167.057		n.i.	0.13 ab	0.12 ab	0.16 ab	0.21 a	0.07 b	0.12 ab
169.164		n.i.	0.04 b	0.04 b	0.09 a	0.11 a	0.03 b	0.04 b
173.157	C10H20O2H+	Butanoic Acid Hexyl Ester*, Octanoic Acid Ethyl Ester*, Decanoic Acid	0.17 a	0.14 a	0.10 a	0.13 a	0.07 a	0.13 a
177.110	C13H21+	n.i.	0.02 abc	0.02 abc	0.03 ab	0.03 a	0.01 c	0.01 bc

257

258 3.2 Fresh-cut processing significantly affects nectarine volatilome

259 Fruit VOC profile of each nectarine cultivar was significantly modified by the fruit
260 processing, as revealed by gas chromatographic (Fig. 1 and Tab. 1) and direct injection (Fig. 2 and
261 Tab. 2) analysis. Based on the principal component analysis (PCA), carried out using the PTR-ToF-
262 MS results (Fig. 2a), the first two principal components accounted for 84 % of total variance. Most
263 of VOC differences between intact and fresh-cut fruit were described by the first principal
264 component (PC1: 67 %), whilst differences between cultivars were mostly explained by the second
265 component (PC2: 17 %). This variation was led by a higher concentration of several VOCs
266 composing the volatile profile of RTE fresh-cut nectarines as shown in the PCA loading plot (Fig.
267 2b) and in the heatmaps of the relative fold changes carried out with either SPME/GC-MS (Fig. 1b)
268 and PTR-ToF-MS results (Fig. 2c). VOCs were significantly grouped into three and four clusters,
269 for SPME/GC-MS and PTR-ToF-MS analysis, respectively (Fig. 1b and 2c). The concentration of
270 each VOC in response to fruit processing varied differently according to the cultivar.
271 Monoterpenes, esters, and aldehydes were the VOC classes mostly affected by fruit fresh-cutting as
272 revealed by both gas chromatographic (Fig. 1) and PTR-ToF-MS (Fig. 2) analysis.

273



274

275 **Figure 1.** Analysis of unprocessed and processed nectarine VOC profile assessed by SPME/GC-MS.

276 The bar plot of panel (a) shows the comparison of the main VOC classes of process and unprocessed fruit of

277 the three nectarine cultivars (August Red, Morsiani 60, Western Red) detected by SPME/GC-MS analysis

278 and reported in detail into the Table 1. Plot (b) represents the heatmap and the hierarchical dendrogram of the

279 fold change (Log (processed/unprocessed)) of VOCs detected by SPME/GC-MS. Cluster analysis was

280 performed using Ward's method on centred data (the high-resolution vector form of the heatmap is

281 illustrated in SFig. 1).

282

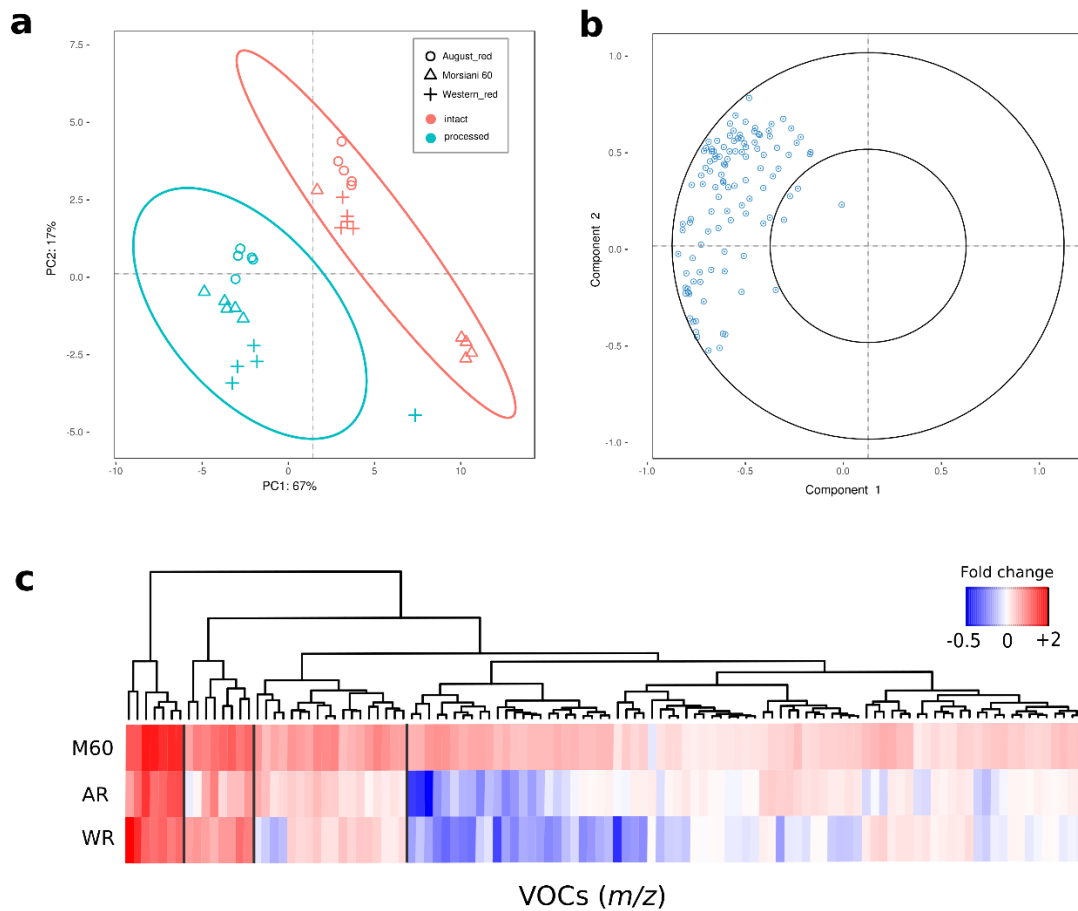
283 The concentration of masses related to monoterpenes (i.e. limonene, linalool, trans-carveol, 4-

284 terpineol, geraniol and β -myrcene), namely m/z 137.134, m/z 93.069, and m/z 95.086, significantly

285 increased after processing in all cultivars. This increase due to processing was mostly evident in AR

286 nectarines (Fig. 2c and Tab. 2). Alteration of the monoterpene volatilome composition, revealed by
287 direct injection assessment by PTR-ToF-MS, was confirmed by SPME/GC-MS. Concentration of
288 limonene increased after processing in all the cultivars, with the strongest fold change for AR
289 (around 50 time higher) followed by WR and M60 (Fig. 1b and Tab. 1). **The increase in**
290 **monoterpenes emission may be the consequence of the mechanical wounding of the fruit, either by**
291 **immediate release of pre-formed compounds sequestered in cellular compartments, or by**
292 **stimulation of the enzymatic pathways leading to VOCs synthesis (Toivonen, 1997).** Noticeable
293 examples are the mevalonic acid and methylerythritol phosphate pathways to produce isopentenyl
294 diphosphate and dimethylallyl diphosphate, as substrates for the activity of the terpene synthases
295 enzyme (Forney, 2016).

296



297

298 **Figure 2.** Analysis of unprocessed and processed nectarine VOC profile assessed by PTR-ToF-MS. Plot (a)
299 depicts the VOC profile distribution of the three nectarine cultivars over the PCA score plot defined by
300 the first two principal components. Plot (b) shows the projection of the VOCs identified by PTR-ToF-
301 MS analysis (the high-resolution vector form of the loading plot is illustrated in SFig 2). Plot (c)
302 represents the heatmap and the hierarchical dendrogram of the fold change (Log
303 (processed/unprocessed)) of VOCs detected by PTR-ToF-MS. Cluster analysis was performed using
304 Ward's method on centred data (the high-resolution vector form of the heatmap is illustrated in SFig.
305 3).

306
307 Different trends of variation in aldehyde emissions were found after fruit processing. RTE
308 fresh-cut nectarines of all cultivars were characterized by an **increased** acetaldehyde (m/z 45.032)
309 emission, that was almost 50 times higher for M60 processed fruit and around 10 times higher for
310 the other two cultivars (Tab. 2 and Fig. 2c). Similarly, butanal (m/z 73.065) concentration was
311 significantly increased by the cutting process, especially for WR and M60 fruit. C6-aldehydes,
312 indicated by m/z 99.080 ((E)-2-hexenal) and m/z 101.096 (hexanal), significantly increased only in
313 RTE fresh-cut fruit of M60 while they remained stable for the other cultivars (Tab. 2 and Fig. 2c).
314 An increase of C6-aldehydes is generally associated with tissue disruption as a typical response to
315 mechanical injury (Aprea et al., 2009), and it is driven by lipoxygenase (LOX) activity (Deza-
316 Durand & Petersen, 2011). Furthermore, C6-aldehydes are part of the signalling network resulting
317 in the activation of plant defences triggered by mechanical damages in plant tissues (Cellini et al.,
318 2018).

319 Aldehydes can be further converted into the associated alcohols through the action of alcohol
320 dehydrogenase (Forney, 2016). Indeed, in our experiment, ethanol (m/z 47.049) concentration
321 significantly increased in fresh cut fruit of the three cultivars proportionally to acetaldehyde
322 enhancement. Moreover, C6-alcohols (m/z 83.086), identified by SPME/GC-MS analysis as (Z)-2-
323 hexen-1-ol and hexanol, significantly increased after processing only for M60 fruit that were also

324 characterized by an increased concentration of C6-aldehyde. Among the remaining alcohols,
325 methanol (m/z 33.033) production was significantly enhanced in fresh-cut fruit of M60 (Tab. 2 and
326 Fig. 2c), most probably originated by the degradation of the cell wall pectin due to cell disruption
327 (Fall and Benson, 1996).

328 After processing, ethyl acetate concentration (m/z 61.028 and m/z 89.059) significantly
329 increased suggesting the conversion of ethanol to the related esters by the action of the alcohol
330 acyltransferase (Balbontín et al., 2010). Tissue disruption by cutting also increased the emission of
331 several other ester compounds mostly represented by the masses m/z 75.044, m/z 117.091, m/z
332 131.1076, and m/z 145.124, tentatively identified as methyl acetate, isobutyl acetate, butyl acetate,
333 isoamyl acetate, amyl acetate, and hexyl acetate (Tab. 2). These esters, commonly related to fruity
334 odours, contribute to the pleasant aroma of nectarines (Rizzolo et al., 2006; Ortiz et al., 2009).
335 Green-odour esters such as (Z)-3-hexenyl acetate and (E)-2-hexenyl acetate (m/z 143,109) were also
336 enhanced in response to fresh-cut processing.

337 Lactones, namely γ -hexalactone (m/z 115.113), γ -octalactone, γ -decalactone, δ -decalactone,
338 and γ -undecalactone were stable after fruit processing in all cultivars (Sab. 1; Tab. 2; Fig. 1).
339 Lactones, which are associated with pleasant and fruity notes (Rizzolo et al., 2006; Zhang et al.,
340 2011), are key contributors to the perceived peach aroma. Therefore, their stability after fruit
341 processing is a desirable trait that may positively affect the aroma of the processed nectarines.

342 One mass related to sulphur-containing compound (m/z 63.029) was detected by PTR-ToF-
343 MS analysis. This mass, putatively identified as dimethyl sulfide, significantly increased after
344 processing and may originate from amino acid breakdown and membrane deterioration. As most of
345 sulfur compounds, dimethyl sulfide can be perceived at relatively low concentration and it can be
346 considered as a strong off-flavour characterized by the cooked, cabbage-like odour (Mussinan &
347 Keelan, 1994).

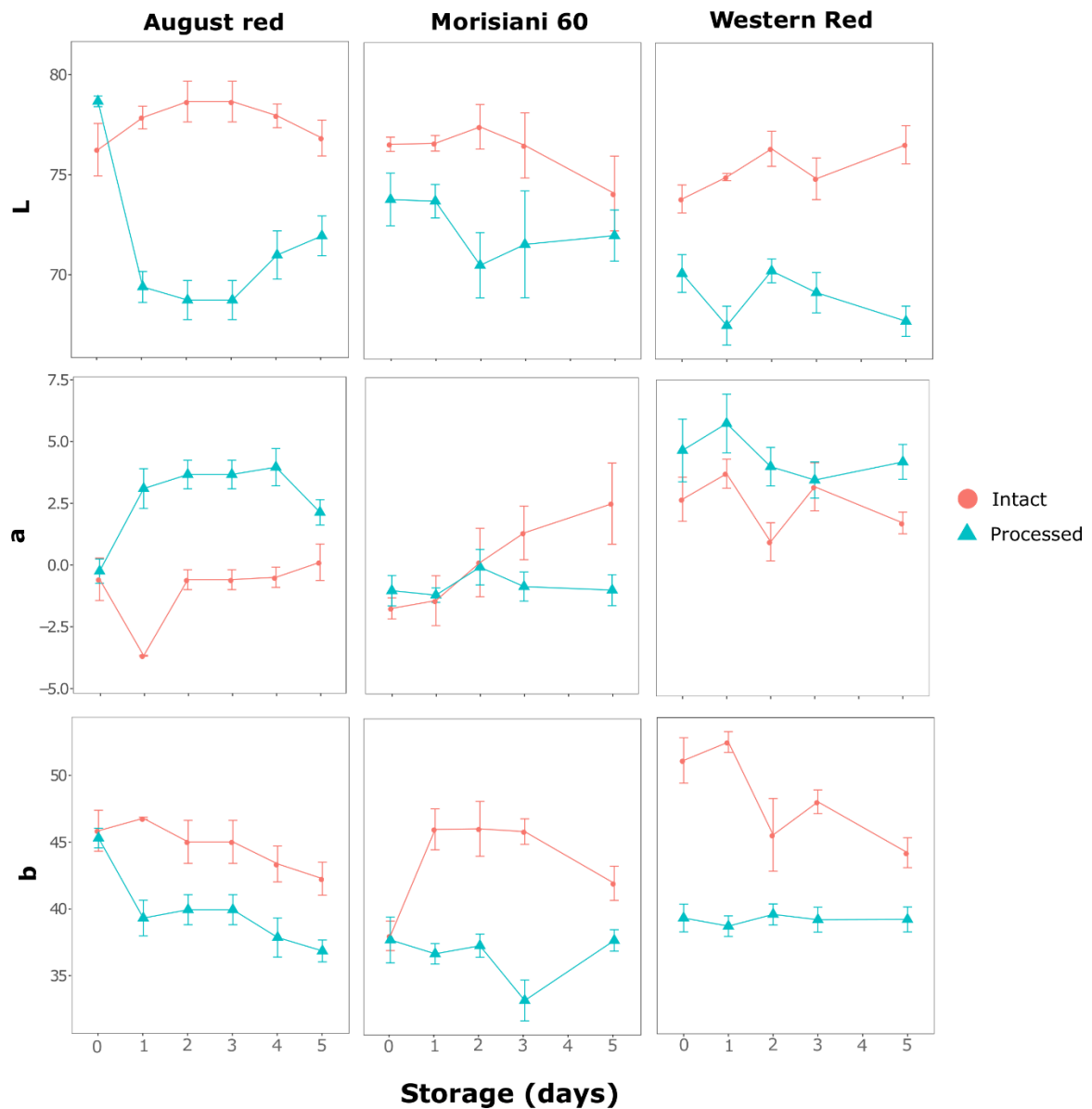
348

349 3.3 Effect of storage duration on fresh-cut nectarine volatiles

350 Fruit processing altered the nectarine colouration resulting in a drop of fruit colour brightness
351 (L^*) in all cultivars (Fig. 3). This variation was maintained over time during postharvest storage.
352 Higher values of a^* (associated with a higher red colour degree of the fruit flesh) were induced by
353 fruit processing in AR and WR, but not in M60 (Fig. 3b). Intact fruit showed higher values of b^* in
354 all cultivars, suggesting a lower yellow intensity of the flesh of fresh-cut fruit (Fig. 3c).
355 Nonetheless, in processed AR and M60 fruit, the reduction of b^* values started only after 1 day of
356 storage. The chroma index, representing colour saturation, is largely affected by b^* . Thus, the cv AR
357 presents a slight discolouration of fruit flesh over time, regardless from the cutting process
358 (Koukounaras et al., 2008; Allegra et al., 2015).

359 Similarly to Giné Bordonaba et al. (2014), any significant surface browning emerged during
360 the five days of cold storage for all three cultivars (SFig. 4), as a possible positive effect of the
361 antioxidant treatment applied to nectarine slices after cutting. Moreover, the dipping of fruit slices
362 may have also **inactivated** from the fruit surface most of the enzymes released during cutting and
363 slicing processes (Soliva-Fortuny & Martín-Belloso, 2003). **However, based on results of Cáceres**
364 **(et al. 2016), the substantial variation of L^* value, measured one day after processing only in AR**
365 **nectarines, can reveal an incipient flesh browning that is higher than the human perception**
366 **threshold.**

367



368

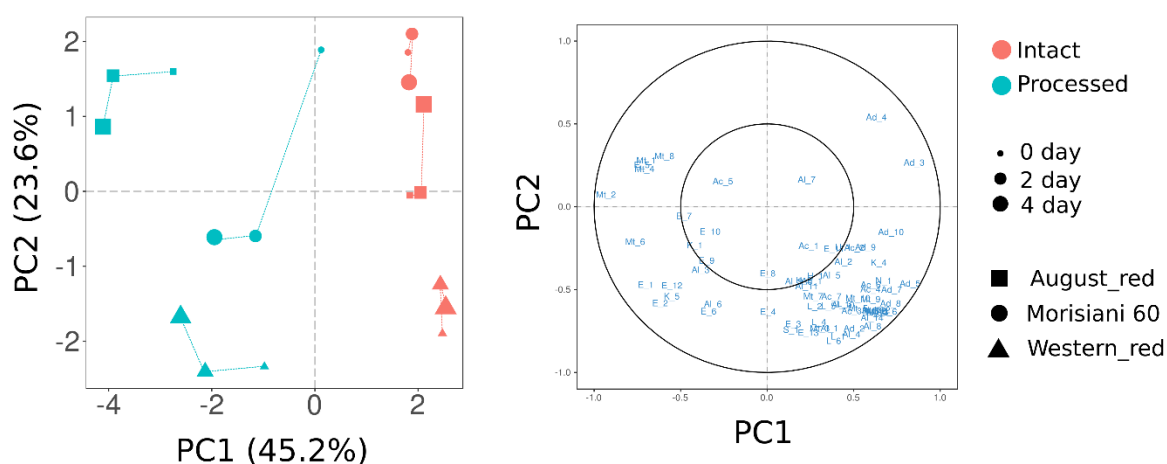
369 **Figure 3.** Chromatic evolution (Lab) during storage (5 d) of unprocessed and fresh-cut nectarine fruit
 370 assessed by tristimulus colorimeter. Each point is the average plus standard deviation of 5 biological
 371 replicates.

372

373 A principal component analysis was carried out on the SPME/GC-MS results to describe the
 374 relative effect of cultivar-dependent features, fruit processing and duration of storage on RTE fresh-
 375 cut volatilome (Fig. 4). Over 68 % of the total variability was described by the first two principal
 376 components. The volatilome of processed nectarines during storage differed substantially from that

377 of intact ones and evolved differently during cold storage according to the cultivar. The first
 378 principal component, explaining 45.2 % of the total variability, mostly revealed differences due to
 379 fruit processing, while the second component (PC2: 23.6 %) mostly differentiated the three
 380 cultivars. Volatile profile of unprocessed nectarines resulted more stable during the storage in
 381 comparison to the fresh-cut fruit. RTE fresh-cut nectarine, indeed, enhanced the concentration of
 382 several esters, mostly ethyl acetate, isobutyl acetate, and isoamyl acetate during storage (loading
 383 plot of Fig. 4 and SFig. 5)

384



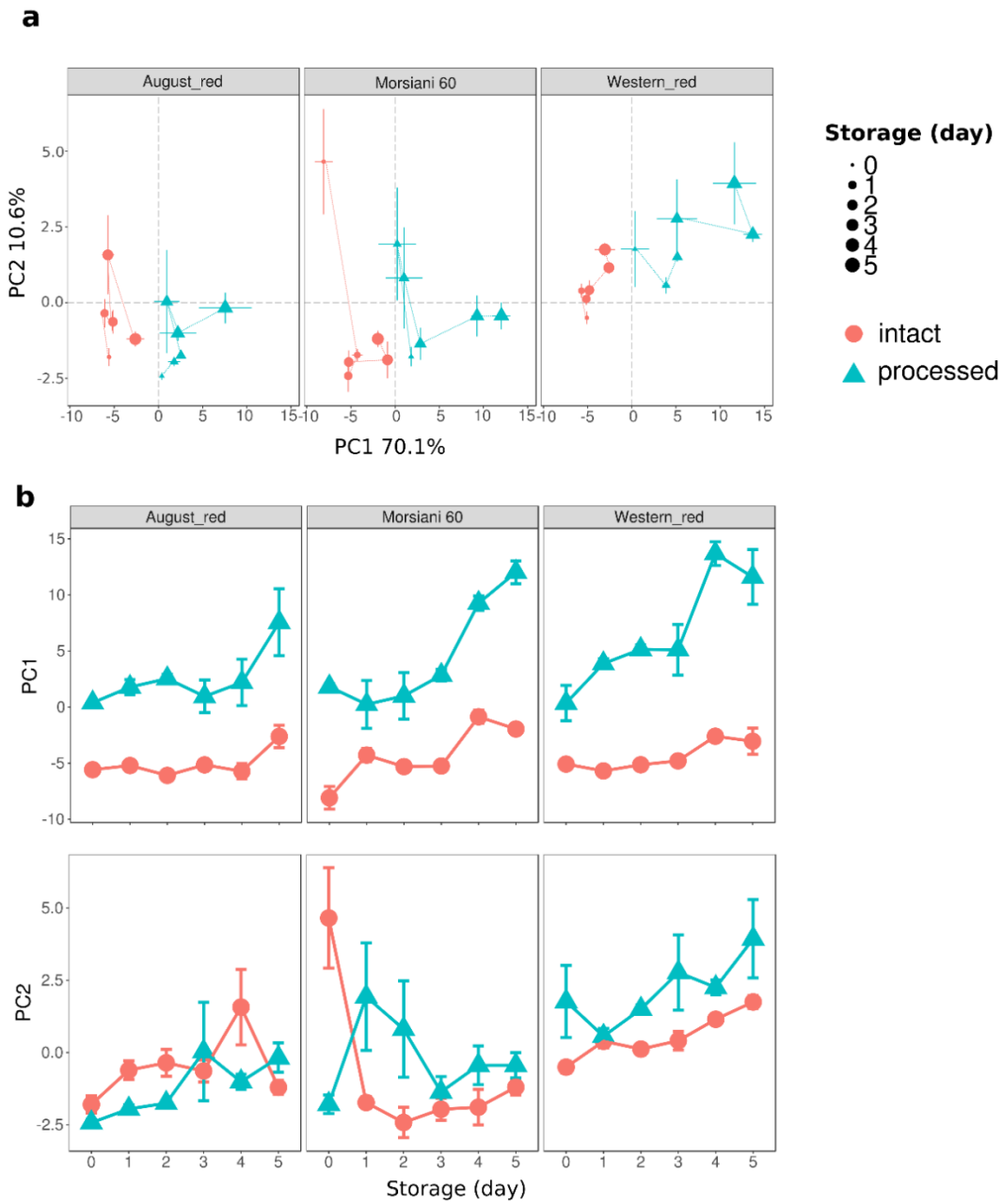
385

386 **Figure 4.** Analysis of unprocessed and fresh-cut nectarine VOC profile during cold storage assessed by
 387 SPME/GC-MS. Plot (a) depicts the VOC profile evolution of the three nectarine cultivars during cold
 388 storage (assessed at day 0, 2, and 4) over the PCA score plot defined by the first two principal
 389 components. Plot (b) shows the projection of the VOCs identified by SPME/GC-MS analysis.

390

391 A principal component analysis was performed also for VOC data obtained by PTR-ToF-MS
 392 (Fig. 5A). Over 80 % of the total variability was described by the first two principal components.
 393 The first principal component (corresponding to 70.1 % of the total variance) mostly discriminated
 394 the VOC emission between intact and processed fruit and the evolution during storage, similarly to
 395 the gas chromatographic analysis. Differences between cultivars were mostly evinced based on the

396 second principal component (10.5 % of the total variance). Since most of the VOC variation in the
 397 nectarine volatilome during cold storage was expressed by these two principal components, values
 398 of PC1 and PC2, extracted from the PCA carried out with all the PTR-ToF-MS data, were
 399 considered as reliable time-related indexes to describe the volatilome evolution during storage (Fig.
 400 5b). The modelling of PC scores to describe time-related alteration of fresh-cut products was
 401 already successfully adopted by Derossi et al. (2016) to estimate fresh-cut lettuce shelf life.
 402



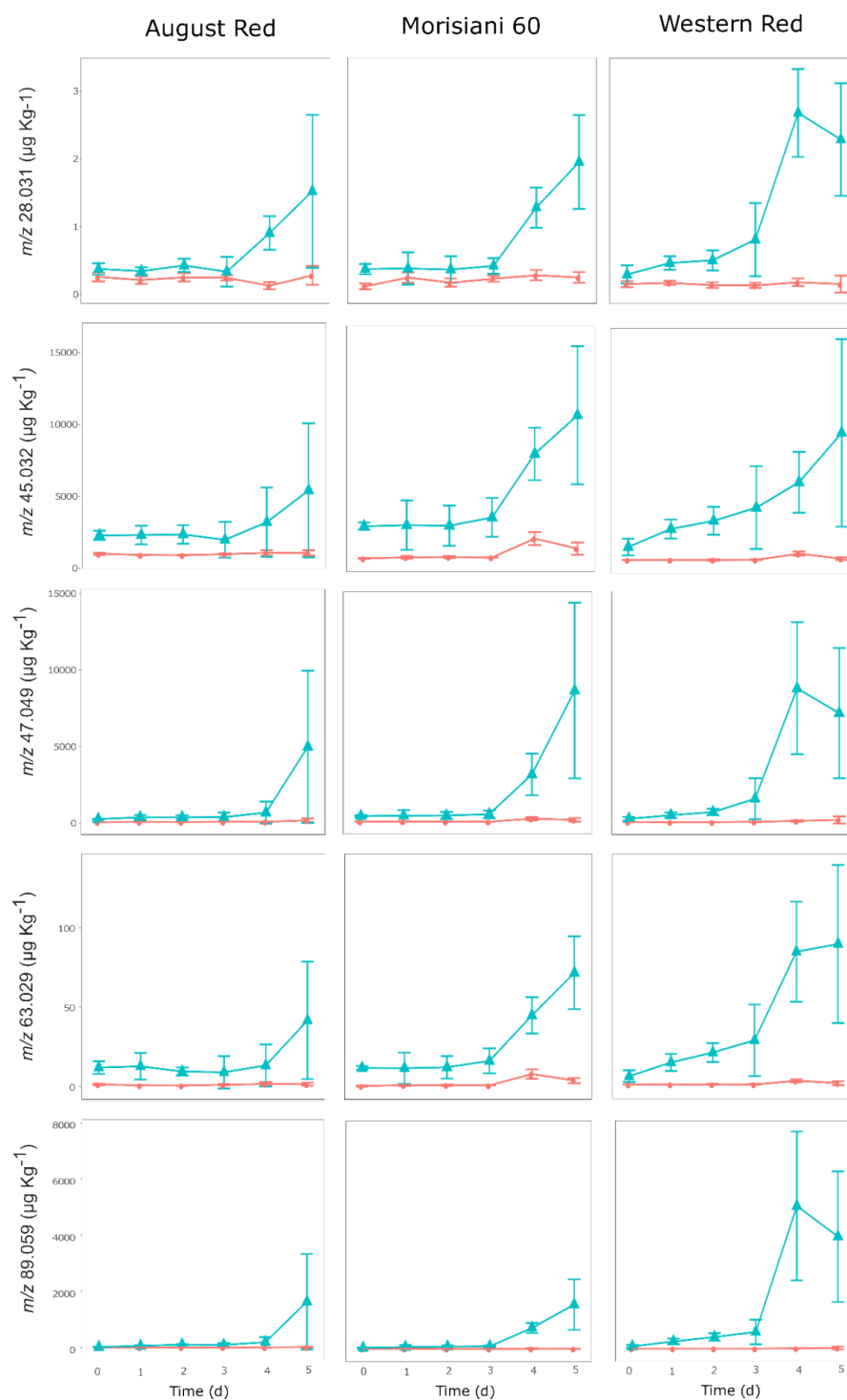
403

404 **Figure 5.** Analysis of unprocessed and processed nectarine VOC profile during cold storage assessed by
405 PTR-ToF-MS. Plot (a) depicts the VOC profile evolution of the three nectarine cultivars during cold
406 storage (daily assessed for 5 d) over the PCA score plot defined by the first two principal components.
407 The high-resolution vector form of the loading plot is illustrated in SFig 6. Plot (b) shows the
408 evolution of PC1 and PC2 scores (extracted from the PCA analysis of Fig. 5a) during the 5 d of
409 storage. Each point is the average plus standard deviation of 5 biological replicates.

410

411 Although not following a definite pattern, the evolution of samples during storage occurs
412 mostly on the second principal component (PC2) variation (Fig. 4b). As previously observed, PC2
413 also allows to discriminate volatilome differences between cultivars in both fresh-cut and
414 unprocessed fruit. Overall differences in **volatile** emission between intact and RTE fresh-cut fruit
415 existed immediately after processing and remained stable until three days of storage, but drastically
416 increased after 4 and/or 5 d of cold storage. On the other hand, unprocessed fruit revealed less
417 marked volatilome alteration during the five days of storage (Fig 5b). The increase of PC1 values in
418 the last days of storage is associated with a pool of VOCs that increased in the same period (Fig. 6
419 and SFig. 7). Most of these compounds are related to fermentative metabolites such as ethanol (m/z
420 47.049) and acetaldehyde (m/z 45.032), but also to the burst in ethylene (m/z 28.031) production
421 (Fig. 6). The accumulation of fermentative metabolites during fruit maturation and senescence
422 induced the synthesis of other aroma volatiles such as acetate esters and ethyl esters (Larsen &
423 Watkins, 1995; Ortiz et al., 2009), as confirmed by the parallel increase of ethyl acetate identified
424 by the molecular masses m/z 89.059 (Fig. 6) and m/z 61.028, methyl acetate (m/z 75.044), and ethyl
425 crotonate (m/z 115.076) (Sfig. 7). Esters are generally associated with fruity and floral aromas and
426 therefore this increase may positively contribute to the pleasant aroma of nectarines. The
427 accumulation of these compounds is common during ripening and can be enhanced by several
428 factors, including chilling injury, temperature, and fermentation, consequent to the exposure of the
429 fruit to low oxygen concentration (Pesis, 2005). In our experimental conditions, the packaging

430 process of fruit slices may have induced a depletion of O₂ and/or an accumulation of CO₂ (Jacxsens
431 et al., 2000), resulting in the production of fermentative off-flavour metabolites causing aroma
432 spoilage during the last days of refrigerated storage. Other off-flavour compounds increased starting
433 from the fourth day of storage in processed fruit, such as dimethyl sulfide (*m/z* 63.029) (fig. 6) and
434 C5 acids (isovaleric acid or pentanoic acid, *m/z* 103.075; Sfig. 7). The variation of the PC1 was also
435 determined by the increase of an array of other VOCs detected by PTR-ToF-MS analysis such as
436 formaldehyde (*m/z* 31.018), 1-butanol (*m/z* 57.07), furan (*m/z* 69.033), 2-methyl-1-butanol (*m/z*
437 71.085), butanal (*m/z* 73.065), 2-methyl-propanol (*m/z* 75.079), butyrolactone (*m/z* 87.044), benzyl
438 alcohol (*m/z* 91.068), and styrene (*m/z* 105.05).



439

440

441 **Figure 6.** Storage evolution of five masses (out of 112 detected in total by PTR-ToF-MS). These masses
 442 have been selected to monitor the fruit spoilage level: ethylene (m/z 28.031), acetaldehyde (m/z
 443 45.032), ethanol (m/z 47.049), dimethyl sulfide (m/z 63.029), and ethyl acetate (m/z 89.059). All data
 444 are shown as the average and standard deviation of 5 biological replicates. The storage evolution of all
 445 the detected masses is reported in the SFig. 7.

446

447 **4. Conclusions**

448 The lack of flavour, caused by incorrect conservation and harvesting practices which are not
449 tailored on each specific cultivar, is one of the main reasons contributing to consumers'
450 dissatisfaction and a decline in the per capita consumption of peaches (Belisle et al., 2017; Cantin et
451 al., 2009). Results of this study revealed that fresh-cut processing induced a substantial variation in
452 the volatile profile of the nectarines through enhancement of different VOC classes, especially for
453 esters and monoterpenes. This volatilome **modification**, due to fresh-cutting, may be considered as a
454 valuable and applicable strategy to enhance peach and nectarine perceived quality and,
455 consequently, consumer satisfaction. **A practical application of the proposed approach is the fast**
456 **massive screening of cultivars, selecting those richer in desired volatile compounds to submit to**
457 **sensory analysis, reducing the efforts and the cost of the sensory evaluation (Corollaro et al 2014).**

458 However, the volatilome of fresh-cut nectarines was less stable during storage, resulting in a
459 shorter shelf-life based on off-flavour emission. Since visual appearance of fresh-cut fruit did not
460 show any significant deterioration during storage, consumers could be misled in the perception of
461 the product quality and freshness at purchase, as surface appearance is the main parameter driving
462 consumers to purchase the fresh-cut fruit. At consumption, the higher concentration of off-flavour
463 metabolites, such as ethanol, acetaldehyde or dimethyl sulfide, could ruin the eating experience,
464 therefore undermining the consumers likelihood of repurchase the product.

465 Thus, a reliable quality management system based on the use of biomarkers is necessary to
466 control RTE fresh-cut product. This comprehensive volatilome investigation based on direct
467 injection analysis (PTR-ToF-MS) and gas chromatographic analysis (SPME/GC-MS) allowed the
468 detection of an array of putative VOC biomarkers that could be used during all stages of the fresh-
469 cut industry: from the selection of the genotypes most suitable for fresh-cutting, to the final
470 prediction of the product spoilage. However, in consideration of the high cost of commercial mass

471 spectrometry equipment, we advise the possible employment of these biomarkers to develop
472 innovative electronic gas sensors (Mascini et al. 2018) and smart labels. The application of smart
473 labelling may play a key role in identifying changes in the headspace of the packaging due to the
474 accumulation of off-flavour volatiles. For instance, smart labels sensitive to ethanol and/or dimethyl
475 sulfide could be used as marker indicating that fruit is incurring in fermentation and therefore to
476 flavour spoilage.

477

478 **Acknowledgement**

479 The authors thank Emanuela Betta for her support in the SPME/GC-MS and Macè s.r.l by making
480 available their industrial facility to process and pack the nectarine fruit. This publication uses data
481 collected within the framework of the PhD thesis “Aroma of peaches and nectarines: interaction
482 between maturity at harvest, postharvest conditions and fresh-cut processing” by Alessandro
483 Ceccarelli published in 2018 at “Alma Mater Studiorum - University of Bologna”.

484

485 **Author contribution**

486 FS and BF conceived the experiment. ID and ACel contributed to design the experiments and
487 performed the classical postharvest analysis. BF and ACec analysed the data and performed the
488 statistical analysis. BF and ACec drafted the manuscript. IK BF and FB processed and analyzed
489 PTR-ToF-MS data. BF and EA processed and analyzed GC-MS data. FS supervised the work. All
490 authors critically contributed to the review of the manuscript and discussion of the data.

491

492 **5. References**

493 Allegra, A., Barone, E., Inglese, P., Todaro, A., & Sortino, G. (2015). Variability of sensory profile
494 and quality characteristics for “ Pesca di Bivona ” and “ Pesca di Leonforte ” peach (Prunus

495 persica Batsch) fresh-cut slices during storage. *Postharvest Biology and Technology*, 110,
496 61–69. <https://doi.org/10.1016/j.postharvbio.2015.07.020>

497 Aprea, E., Biasioli, F., Carlin, S., Endrizzi, I., & Gasperi, F. (2009). Investigation of Volatile
498 Compounds in Two Raspberry Cultivars by Two Headspace Techniques: Solid-Phase
499 Microextraction/Gas Chromatography-Mass Spectrometry (SPME/GC-MS) and Proton-
500 Transfer Reaction-Mass Spectrometry (PTR-MS). *J. Agric. Food Chem.* 57, 4011–4018.
501 <https://doi.org/10.1021/jf803998c>.

502 Artés, F. & Gómez, P.A., 2006. Physical, physiological and microbial deterioration of minimally
503 fresh processed fruits and vegetables. *Food Science and Technology International*, 13(3),
504 177–188. <https://doi.org/10.1177/10820132013207079610>.

505 Balbontín, C., Gaete-Eastman, C., Fuentes, L., Figueroa, C.R., Herrera, R., Manriquez, D., Latché,
506 A., Pech, J.C., Moya-León, M.A. (2010). VpAAT1, a gene encoding an alcohol
507 acyltransferase, is involved in ester biosynthesis during ripening of mountain papaya fruit. *J.*
508 *Agric. Food Chem.* 58, 5114–5121. doi:10.1021/jf904296c

509 Beaulieu, J.C. and Baldwin E.A. (2002). Flavor and aroma of fresh-cut fruits and vegetables. In
510 book: *Fresh-cut fruits and Vegetables. Science, technology and market.* Publisher: CRC Press
511 LLC. Editor: lamikanra O.

512 Belisle, C., Adhikari, K., Chavez, D., & Phan, U. T. X. (2017). Development of a lexicon for flavor
513 and texture of fresh peach cultivars. *Journal of Sensory Studies*, 32(4), e12276.
514 <https://doi.org/10.1111/joss.12276>

515 Bianchi, T., Weesepeol, Y., Koot, A., Iglesias, I., Eduardo, I., Gratacós-cubarsí, M., Guerrero, L.,
516 Hortós, M., Ruth, S. Van (2017). Investigation of the aroma of commercial peach (*Prunus*
517 *persica* L . Batsch) types by Proton Transfer Reaction – Mass Spectrometry (PTR-MS) and
518 sensory analysis. *Food Research International*, 99, 133–146.
519 <https://doi.org/10.1016/j.foodres.2017.05.007>.

- 520 Bonora, E., Noferini, M., Stefanelli, D., & Costa, G. (2014). A new simple modeling approach for
521 the early prediction of harvest date and yield in nectarines. *Scientia Horticulturae*, 172, 1–9.
522 <https://doi.org/10.1016/j.scienta.2014.03.030>.
- 523 Brizzolara, S., Hertog, M., Tosetti, R., Nicolai, B. & Tonutti, P. (2018). Metabolic responses to
524 low temperature of three peach fruit cultivars differently sensitive to cold storage. *Frontiers in*
525 *Plant Science*. <https://doi.org/10.3389/fpls.2018.00706>.
- 526 Cáceres, D., Díaz, M., Shinya, P., Infante, R. (2016). Assessment of peach internal flesh browning
527 through colorimetric measures. *Postharvest Biology and Technology*, 111, 48-52.
528 <https://doi.org/10.1016/j.postharvbio.2015.07.007>
- 529 Cano-Salazar, J., López, M. L., Crisosto, C. H., & Echeverría, G. (2013). Volatile compound
530 emissions and sensory attributes of “Big Top” nectarine and “Early Rich” peach fruit in
531 response to a pre-storage treatment before cold storage and subsequent shelf-life. *Postharvest*
532 *Biology and Technology*, 76, 152–162. <https://doi.org/10.1016/j.postharvbio.2012.10.001>
- 533 Cantin, C.M., Torrents, J., Gogorcena, Y., Moreno M.A. (2009). Fruit quality attributes of new
534 peach and nectarine varieties under selection in the ~~ebro~~-Ebro valley conditions (Spain). *Acta*
535 *horticulturae* 814(814):493-500. DOI: 10.17660/ActaHortic.2009.814.83
- 536 Capozzi, V., Yener, S., Khomenko, I., Farneti, B., Cappellin, L., Gasperi, F., Scampicchio, M.,
537 Biasioli, F. (2017). PTR-ToF-MS Coupled with an Automated Sampling System and Tailored
538 Data Analysis for Food Studies: Bioprocess Monitoring, Screening and Nose-space Analysis.
539 *Journal of Visualized Experiments : JoVE*, (123). <https://doi.org/10.3791/54075>.
- 540 Cappellin, L., Biasioli, F., Granitto, P. M., Schuhfried, E., Soukoulis, C., Costa, F., Märk, T. D.,
541 Gasperi, F. (2011a). On data analysis in PTR-TOF-MS: From raw spectra to data mining.
542 *Sensors and Actuators B: Chemical*, 155(1), 183–190.
543 <https://doi.org/10.1016/j.snb.2010.11.044>.
- 544 Cappellin, L., Biasioli, F., Schuhfried, E., Soukoulis, C., Märk, T. D., & Gasperi, F. (2011b).

545 Extending the dynamic range of proton transfer reaction time-of-flight mass spectrometers by a
546 novel dead time correction. *Rapid Communications in Mass Spectrometry : RCM*, 25(1), 179–
547 83. <https://doi.org/10.1002/rcm.4819>.

548 Cavaiuolo, M., Cocetta, G., Bulgari, R., Spinardi, A., & Ferrante, A. (2015). Identification of
549 innovative potential quality markers in rocket and melon fresh-cut produce. *Food Chemistry*,
550 188, 225–233. <https://doi.org/10.1016/J.FOODCHEM.2015.04.143>.

551 Ceccarelli, A. (2018). Aroma of peaches and nectarines: interaction between maturity at harvest,
552 postharvest conditions and fresh-cut processing, [Dissertation thesis], Alma Mater Studiorum
553 Università di Bologna. Dottorato di ricerca in Scienze e tecnologie agrarie, ambientali e
554 alimentari. DOI 10.6092/unibo/amsdottorato/8423.

555 Cellini, A., Buriani, G., Rocchi, L., Rondelli, E., Savioli, S., Rodriguez Estrada, M.T., Cristescu,
556 S.M., Costa, G., Spinelli, F. (2018). Biological relevance of volatile organic compounds
557 emitted during the pathogenic interactions between apple plants and *Erwinia amylovora*.
558 *Molecular Plant Pathology*, 19(1), 158-168. doi: 10.1111/mpp.12509

559 Colantuono, F., Amodio M.L., Piazzolla, F., Colelli, G. (2012). Influence of quality attributes of
560 early, intermediate and late peach varieties on suitability as fresh-convenience products.
561 *Advances in horticultural science*, 26(1), 32-38.

562 Corollaro, M. L., Aprea, E., Endrizzi, I., Betta, E., Demattè, M. L., Charles, M., Bergamaschi, M.,
563 Costa, F., Biasioli, F., Corelli Grappadelli L., Gasperi, F. (2014). A combined sensory-
564 instrumental tool for apple quality evaluation. *Postharvest Biology and Technology*, 96, 135–
565 144. <https://doi.org/10.1016/j.postharvbio.2014.05.016>

566 Denoya, G. I., Polenta, G. A., Apóstolo, N. M., Budde, C. O., Sancho, A. M., & Vaudagna, S. R.
567 (2016). Optimization of high hydrostatic pressure processing for the preservation of minimally
568 processed peach pieces. *Innovative Food Science & Emerging Technologies*, 33, 84–93.
569 <https://doi.org/10.1016/j.ifset.2015.11.014>.

- 570 Denoya, G. I., Vaudagna, S. R., Godoy, M. F., Budde, C. O., & Polenta, G. A. (2017). Suitability of
571 different varieties of peaches for producing minimally processed peaches preserved by high
572 hydrostatic pressure and selection of process parameters. *LWT - Food Science and Technology*,
573 78, 367–372. <https://doi.org/10.1016/j.lwt.2017.01.006>.
- 574 Denoya, G. I., Vaudagna, S. R., & Polenta, G. (2015). Effect of high pressure processing and
575 vacuum packaging on the preservation of fresh-cut peaches. *LWT - Food Science and*
576 *Technology*, 62(1), 801–806. <https://doi.org/10.1016/j.lwt.2014.09.036>.
- 577 Derossi, A., Mastrandrea, L., Amodio, M. L., de Chiara, M. L. V., & Colelli, G. (2016). Application
578 of multivariate accelerated test for the shelf life estimation of fresh-cut lettuce. *Journal of*
579 *Food Engineering*, 169, 122–130. <https://doi.org/10.1016/J.JFOODENG.2015.08.010>.
- 580 Deza-Durand, K. M., & Petersen, M. A. (2011). The effect of cutting direction on aroma
581 compounds and respiration rate of fresh-cut iceberg lettuce (*Lactuca sativa* L.). *Postharvest*
582 *Biology and Technology*, 61(1), 83–90. <https://doi.org/10.1016/j.postharvbio.2011.02.011>.
- 583 Eduardo, I., Chietera, G., Bassi, D., Rossini, L., & Vecchietti, A. (2010). Identification of key odor
584 volatile compounds in the essential oil of nine peach accessions. *Journal of the Science of*
585 *Food and Agriculture*, 90(7), 1146–54. <https://doi.org/10.1002/jsfa.3932>.
- 586 Eissa, H. A., Fadel, H. H. M., Ibrahim, G. E., Hassan, I. M., & Elrashid, A. A. (2006). Thiol
587 containing compounds as controlling agents of enzymatic browning in some apple products.
588 *Food Research International*, 39(8), 855–863. <https://doi.org/10.1016/j.foodres.2006.04.004>.
- 589 Fall, R., & Benson, A. A. (1996). Leaf methanol — the simplest natural product from plants.
590 *Trends in Plant Science*, 1(9), 296–301. [https://doi.org/10.1016/S1360-1385\(96\)88175-0](https://doi.org/10.1016/S1360-1385(96)88175-0).
- 591 Farneti, B., Busatto, N., Khomenko, I., Cappellin, L., Gutierrez, S., Spinelli, F., Velasco, R.,
592 Biasioli, F., Costa, G., Costa, F. (2014). Untargeted metabolomics investigation of volatile
593 compounds involved in the development of apple superficial scald by PTR-ToF-MS.
594 *Metabolomics*, 11(2), 341–349. <https://doi.org/10.1007/s11306-014-0696-0>.

595 Farneti, B., Gutierrez, M.S., Novak, B., Busatto, N., Ravaglia, D., Spinelli, F., Costa, G. (2015a).
596 Use of the index of absorbance difference (IAD) as a tool for tailoring post-harvest 1-MCP
597 application to control apple superficial scald. *Scientia Horticulturae*, 190, 110-116.
598 <https://doi.org/10.1016/j.scienta.2015.04.023>.

599 Farneti, B., Khomenko, I., Cappellin, L., Ting, V., Romano, A., Biasioli, F., Costa, G., Costa, F.
600 (2015b). Comprehensive VOC profiling of an apple germplasm collection by PTR-ToF-MS.
601 *Metabolomics* 11, 838–850. doi:10.1007/s11306-014-0744-9.

602 Farneti, B., Di Guardo, M., Khomenko, I., Cappellin, L., Biasioli, F., Velasco, R., Costa, F. (2017).
603 Genome-wide association study unravels the genetic control of the apple volatilome and its
604 interplay with fruit texture. *Journal of Experimental Botany*, 68(7), 1467–1478.
605 <https://doi.org/10.1093/jxb/erx018>.

606 Forney, C. F. (2016). Physiology and biochemistry of aroma and off-odors in fresh-cut products.
607 *Acta Horticulturae*, 1141, 35–46. <https://doi.org/10.17660/ActaHortic.2016.1141.4>.

608 Giné Bordonaba, J., Cantin, C. M., Larrigaudière, C., López, L., López, R., & Echeverria, G.
609 (2014). Suitability of nectarine cultivars for minimal processing: The role of genotype, harvest
610 season and maturity at harvest on quality and sensory attributes. *Postharvest Biology and*
611 *Technology*, 93, 49–60. <https://doi.org/10.1016/j.postharvbio.2014.02.007>.

612 Jacxsens, L., Devlieghere, F., De Rudder, T. & Debevere, J. (2000). Designing equilibrium
613 modified atmosphere packages for fresh-cut vegetables subjected to changes in temperature.
614 *LWT - Food Science and Technology*, 33(3), 178-187. <https://doi.org/10.1006/fstl.2000.0639>.

615 Koukounaras, A., Diamantidis, G., & Sfakiotakis, E. (2008). The effect of heat treatment on quality
616 retention of fresh-cut peach. *Postharvest Biology and Technology*, 48, 30–36.
617 <https://doi.org/10.1016/j.postharvbio.2007.09.011>.

618 Larsen, M., & Watkins, C. B. (1995). Firmness and concentrations of acetaldehyde, ethyl acetate
619 and ethanol in strawberries stored in controlled and modified atmospheres. *Postharvest*

620 *Biology and Technology*, 5(1–2), 39–50. [https://doi.org/10.1016/0925-5214\(94\)00012-H](https://doi.org/10.1016/0925-5214(94)00012-H).

621 Lavilla, T., Recasens, I., Lopez, M. L., & Puy, J. (2002). Multivariate analysis of maturity stages,
622 including quality and aroma, in “Royal Glory” peaches and “Big Top” nectarines. *Journal of*
623 *the Science of Food and Agriculture*, 82(15), 1842–1849. <https://doi.org/10.1002/jsfa.1268>.

624 Mascini, M., Gaggiotti, S., Della Pelle, F., Di Natale, C., Qakala, S., Iwuoha, E., Pittia, P.,
625 Compagnone, D. (2018). Peptide Modified ZnO Nanoparticles as Gas Sensors Array for
626 Volatile Organic Compounds (VOCs). *Frontiers in Chemistry*, doi:
627 10.3389/fchem.2018.00105.

628 **Mendoza-Enano, M. L., Stanley, R., & Frank, D. (2019). Linking consumer sensory acceptability to**
629 **volatile composition for improved shelf-life: A case study of fresh-cut watermelon (*Citrullus***
630 **lanatus). *Postharvest Biology and Technology*, 154, 137-147.**
631 **<https://doi.org/10.1016/j.postharvbio.2019.03.018>**

632 Mohammad, A., Rafiee, S., Emam-Djomeh, Z., & Keyhani, A. (2008). Kinetic Models for Colour
633 Changes in Kiwifruit Slices During Hot Air Drying. *World Journal of Agricultural Sciences*,
634 4(3), 376–383. Retrieved from file:///C:/Users/Lg x120/Downloads/15-libre.pdf

635 Mussinan, C.J. and Keelan, M.,E. (1994). Sulfur Compounds in Foods (ACS Symposium Series
636 564). *ACS Symposium Series; American Chemical Society*, 1–6. [https://doi.org/10.1021/bk-](https://doi.org/10.1021/bk-1994-0564.ch001)
637 1994-0564.ch001

638 Mustafa, F., Andreescu S. (2018). Chemical and biological sensors for food-quality monitoring and
639 smart packaging. *Foods*, 7(10), 168. <https://doi.org/10.3390/foods7100168>.

640 Ortiz, A., Echeverria, G., Graell, J., Lara, I. (2009). Overall quality of ‘Rich Lady’ peach fruit after
641 air- or CA storage. The importance of volatile emission. *LWT - Food Science and*
642 *Technology*, 42, 1520-1529. <https://doi.org/10.1016/j.lwt.2009.04.010>.

643 Pesis, E. (2005). The role of the anaerobic metabolites, acetaldehyde and ethanol, in fruit ripening,
644 enhancement of fruit quality and fruit deterioration. *Postharvest Biology and Technology*,

645 37(1), 1–19. <https://doi.org/10.1016/j.postharvbio.2005.03.001>.

646 Pizato, S., Cortez-Vega, W. R., De Souza, J. T. A., Prentice-Hernández, C., & Borges, C. D. (2013).
647 Effects of Different Edible Coatings in Physical, Chemical and Microbiological Characteristics
648 of Minimally Processed Peaches (*Prunus persica* L. Batsch). *Journal of Food Safety*, 33(1),
649 30–39. <https://doi.org/10.1111/jfs.12020>.

650 Rizzolo, A., Zerbini, P. E., Grassi, M., Cambiaghi, P., & Bianchi, G. (2006). Effect of
651 Methylcyclopropene on aroma compounds in Big Top nectarines after shelf life. *Journal of*
652 *Food Quality*, 29(2), 184–202. <https://doi.org/10.1111/j.1745-4557.2006.00066.x>.

653 Soliva-Fortuny, R. C., & Martín-Belloso, O. (2003). New advances in extending the shelf-life of
654 fresh-cut fruits: A review. *Trends in Food Science and Technology*, 14(9), 341–353.
655 [https://doi.org/10.1016/S0924-2244\(03\)00054-2](https://doi.org/10.1016/S0924-2244(03)00054-2).

656 Solomos, T. (1994). Some Biological and Physical Principles Underlying Modified Atmosphere
657 Packaging. In *Minimally Processed Refrigerated Fruits & Vegetables* (pp. 183–225). Boston,
658 MA: Springer US. https://doi.org/10.1007/978-1-4615-2393-2_5

659 Toivonen, P. M. A. (1997). Non-ethylene, non-respiratory volatiles in harvested fruits and
660 vegetables: Their occurrence, biological activity and control. *Postharvest Biology and*
661 *Technology*, 12(2), 109–125. [https://doi.org/10.1016/S0925-5214\(97\)00048-3](https://doi.org/10.1016/S0925-5214(97)00048-3).

662 Varoquaux, P., & Wiley, R. C. (2017). Biological and Biochemical Changes in Minimally
663 Processed Refrigerated Fruits and Vegetables (pp. 153–186). Springer, Boston, MA.
664 https://doi.org/10.1007/978-1-4939-7018-6_5.

665 Wang, Y., Yang, C., Li, S., Yang, L., Wang, Y., Zhao, J., & Jiang, Q. (2009). Volatile
666 characteristics of 50 peaches and nectarines evaluated by HP-SPME with GC-MS. *Food*
667 *Chemistry*, 116(1), 356–364. <https://doi.org/10.1016/j.foodchem.2009.02.004>

668 Yang, D. S., Balandrán-Quintana, R. R., Ruiz, C. F., Toledo, R. T., & Kays, S. J. (2009). Effect of
669 hyperbaric, controlled atmosphere, and UV treatments on peach volatiles. *Postharvest Biology*

670 *and Technology*, 51(3), 334–341. <https://doi.org/10.1016/j.postharvbio.2008.09.005>.
671 Zhang, B., Xi, W. P., Wei, W. W., Shen, J. Y., Ferguson, I., & Chen, K. S. (2011). Changes in
672 aroma-related volatiles and gene expression during low temperature storage and subsequent
673 shelf-life of peach fruit. *Postharvest Biology and Technology*, 60(1), 7–16.
674 <https://doi.org/10.1016/j.postharvbio.2010.09.012>.

675

676

677 **Captions supplementary material**

678

679 **SFigure 1.** High-resolution vector form of the heatmap illustrated in Fig. 1b.

680 **SFigure 2.** High resolution vector form of the loading plot illustrated in Fig. 2b.

681 **SFigure 3.** High-resolution vector form of the heatmap illustrated in Fig. 2c.

682 **SFigure 4.** Browning index evolution of fresh-cut nectarine fruit during storage.

683 **SFigure 5.** VOC differences of unprocessed and fresh-cut nectarine fruit assessed by SPME/GC-
684 MS analysis during storage. Data are reported as relative percentage content.

685 **SFigure 6.** High-resolution vector form of the loading plot of the PCA illustrated in Fig. 4a.

686 **SFigure 7.** VOC differences of unprocessed and fresh-cut nectarine fruit assessed by PTR-ToF-MS
687 analysis during storage. All data concentration ($\mu\text{g kg}^{-1}$) are shown as the average and
688 standard deviation of 5 biological replicates

689